



A refined regional modeling approach for the Corn Belt – Experiences and recommendations for large-scale integrated modeling



Yiannis Panagopoulos^{a,*}, Philip W. Gassman^a, Manoj K. Jha^b, Catherine L. Kling^a, Todd Campbell^a, Raghavan Srinivasan^c, Michael White^d, Jeffrey G. Arnold^d

^a Center for Agricultural and Rural Development, Iowa State University, Ames, IA 50011-1070, USA

^b Civil Engr. Dept., North Carolina A&T State University, 1601 E. Market St., Greensboro, NC 27410, USA

^c Spatial Sciences Laboratory, Texas A&M Univ., College Station, TX 77845, USA

^d USDA-ARS, Grassland, Soil and Water Research Laboratory, Temple, TX 76502, USA

ARTICLE INFO

Article history:

Received 7 July 2014

Received in revised form 12 January 2015

Accepted 20 February 2015

Available online 7 March 2015

This manuscript was handled by Laurent Charlet, Editor-in-Chief, with the assistance of Nicolas Gratiot, Associate Editor

Keywords:

Corn Belt

Large-scale calibration

Nonpoint source pollution

Refined modeling

SWAT

SUMMARY

Nonpoint source pollution from agriculture is the main source of nitrogen and phosphorus in the stream systems of the Corn Belt region in the Midwestern US. This region is comprised of two large river basins, the intensely row-cropped Upper Mississippi River Basin (UMRB) and Ohio-Tennessee River Basin (OTRB), which are considered the key contributing areas for the Northern Gulf of Mexico hypoxic zone according to the US Environmental Protection Agency. Thus, in this area it is of utmost importance to ensure that intensive agriculture for food, feed and biofuel production can coexist with a healthy water environment. To address these objectives within a river basin management context, an integrated modeling system has been constructed with the hydrologic Soil and Water Assessment Tool (SWAT) model, capable of estimating river basin responses to alternative cropping and/or management strategies. To improve modeling performance compared to previous studies and provide a spatially detailed basis for scenario development, this SWAT Corn Belt application incorporates a greatly refined subwatershed structure based on 12-digit hydrologic units or 'subwatersheds' as defined by the US Geological Service. The model setup, calibration and validation are time-demanding and challenging tasks for these large systems, given the scale intensive data requirements, and the need to ensure the reliability of flow and pollutant load predictions at multiple locations. Thus, the objectives of this study are both to comprehensively describe this large-scale modeling approach, providing estimates of pollution and crop production in the region as well as to present strengths and weaknesses of integrated modeling at such a large scale along with how it can be improved on the basis of the current modeling structure and results. The predictions were based on a semi-automatic hydrologic calibration approach for large-scale and spatially detailed modeling studies, with the use of the Sequential Uncertainty Fitting algorithm (SUFI-2) and the SWAT-CUP interface, followed by a manual water quality calibration on a monthly basis. The refined modeling approach developed in this study led to successful predictions across most parts of the Corn Belt region and can be used for testing pollution mitigation measures and agricultural economic scenarios, providing useful information to policy makers and recommendations on similar efforts at the regional scale.

© 2015 Elsevier B.V. All rights reserved.

1. Introduction

Elevated concentrations of Nitrogen (N) and Phosphorus (P) contribute to the water quality impairment of many streams and rivers in the United States. In addition to local impairments, these nutrients contribute to eutrophication in downstream lakes, bays

* Corresponding author at: Center for Agricultural and Rural Development, Iowa State University, Ames, IA 50011-1070, USA. Tel.: +1 515 294 1620.

E-mail address: ypanag@iastate.edu (Y. Panagopoulos).

and estuaries, and are primarily responsible for hypoxia in the Gulf of Mexico (USEPA, 2000, 2007). Under recommendations of the Clean Water Action Plan in 1998, the US Environmental Protection Agency (USEPA) developed a national strategy for establishing water body-specific nutrient criteria for all water bodies (USEPA, 1998) to reduce nutrient concentrations and improve the beneficial ecological uses of surface waters. The Mississippi River/Gulf of Mexico Watershed Nutrient Task Force (2008) established a goal to reduce the size of the hypoxic zone in the Gulf of Mexico to 5000 km², which has been documented to form on a

seasonal basis in most years since 1985 (Rabalais et al., 2007; Turner et al., 2008). This will require substantial reductions in nutrient loadings from the Mississippi/Atchafalaya River basin (MARB) and especially from its most upstream and intensively cultivated region, the 492,000 km² Upper Mississippi River Basin (UMRB) and the 528,000 km² Ohio-Tennessee River Basin (OTRB), which form the ‘Corn Belt’ Region of the US extended across 12 States of the Midwest. The level of nutrient reduction from these basins required to achieve the goal of 5000 km² hypoxic zone has been estimated at 45% (EPA-SAB, 2007).

Agricultural nonpoint source pollution is the main source of N and P discharged to the UMRB and OTRB stream systems, primarily via fertilizer and/or livestock manure applied to cropland or pasture, although point sources are also important nutrient sources. Specifically, these two basins contribute about 82% of the nitrate-N (NO₃-N), 69% of the total Kjeldahl nitrogen (TKN), and 58% of the total P fluxes to the Gulf despite representing only 31% of the total drainage area (EPA-SAB, 2007). On the other hand, the UMRB and OTRB areas are the primary agricultural landscapes of the country with substantial importance for both the regional and national economies. Apart from the required food and feed production from the growing of corn and soybean, there is an ambitious target of biofuel production to be achieved by 2022, either as grain-based ethanol or from cellulosic feedstock, which will further increase the economic importance of the region (USDA Biofuels Strategic Production Report, 2010). Obviously, within this large area, trade-offs between the interdependent goals of food and feed production, sustainable biofuel production, and improved water quality will have significant implications for commodity groups, individual producers and other stakeholders in the region. These implications should also be investigated by considering possible future changes in climate, which will influence management planning.

Within this context, the appropriate use of process-based eco-hydrological models for the evaluation of agricultural management options with socio-economic and environmental impacts under climate variability is crucial. A great advantage of such models is their distributed nature, which is considered indispensable in identifying and prioritizing cost-effective management actions toward multiple targets. In order to reliably address what-if scenarios, however, extensive calibration of these models using measured data at multiple locations is necessary. The development and validation of these models become even more challenging at the regional scale, because of the considerably large input data and computational resource requirements. Although calibration and validation guidelines are increasingly developed to facilitate the use of such models (Moriassi et al., 2012), manual calibration of a distributed watershed model such as the Soil and Water Assessment Tool (SWAT) watershed-scale water quality model (Arnold et al., 1998; Williams et al., 2008), is difficult and time consuming for large-scale applications (Arnold et al., 2012).

SWAT has proven to be an effective tool for evaluating agricultural management simulations for complex landscapes and varying climate regimes (e.g., see Gassman et al., 2007, 2014; Douglas-Mankin et al., 2010; Tuppard et al., 2011). To date, SWAT has already been applied for several studies in the UMRB and to a lesser extent in the OTRB, including studies describing model performance evaluations and calibration/validation approaches (Kannan et al., 2008; Srinivasan et al., 2010; Santhi et al., 2008, 2014), climate change effects on hydrology and water quality (Jha et al., 2006, 2013; Wu et al., 2012a) and evaluation of land use, best management practice (BMP) scenarios and conservation practices (Rabotyagov et al., 2010; Santhi et al., 2014; Secchi et al., 2011; Demissie et al., 2012; Wang et al., 2011; Wu et al., 2012b; White et al., 2014). To maintain modeling efficiency at the regional scale and the feasibility of manual calibration in particular, the

delineation of existing UMRB and OTRB SWAT models into subwatersheds was based on 8-digit Hydrologic Unit Codes (HUCs) or “8-digit watersheds” (USGS, 2012, 2014a). Given the relatively large average area of an 8-digit watershed in these regions (~3600 km²) and the fact that only one set of climate data can be input per subwatershed in SWAT, such an approach needs climate adjustments for each 8-digit watershed, resulting in data inaccuracies with respect to climate spatial variability, the major driving force of hydrological processes, water balance and subsequently water quality estimations across the basin. On the other hand, the use of 12-digit subwatersheds (USGS, 2012, 2014a), which average roughly about 85 km² in area (each 8-digit watershed is comprised of about 40–45 12-digit watersheds – see Fig. 1 as an example) provides the opportunity to more directly and accurately capture meteorological inputs from the thousands of available stations in the Corn Belt, which could not be used in the model with a coarse 8-digit delineation. Any adjustments of the available climate data to derive the ‘average’ climate of a virtual station for a particular 8-digit watershed in this case is not as representative as using directly all the available information across the basin and assigning it to smaller areas of increased hydrologic homogeneity. A great advantage of using a large number of smaller subbasins in a SWAT project is also the consideration of topography in the calculations. SWAT calculates a single slope for each subbasin based on the elevation layer inserted at the beginning of a model’s setup and uses this value by default for all HRUs within each subbasin. By using the more detailed 12-digit watershed delineation, slope differentiation is more accurate across the basin with positive expected impact on the estimation of water balance components (e.g. surface and lateral flow), erosion calculation and water quality predictions. Moreover, such a 12-digit delineation approach in this large modeling system would obviously allow in the future for increased flexibility in defining reservoirs, wetlands and other hydrologic elements close to their real locations, improved representation of river water routing processes at a small time step (daily), more accurate targeting of practices across the landscape as well as linkages to climate data and downscaled Global Climate Model (GCM) projections across a dense grid in a given SWAT simulation.

To be able to address all these issues in an extensive future scenario research in the Corn Belt, we have constructed a SWAT-based modeling system using 12-digit subwatersheds, which can estimate nutrient loads from the UMRB and OTRB regions. The system has already provided the flexibility to analyse a wide range of alternative cropping, management strategies, and/or future climate change scenarios and their impacts on water quality and the hypoxic zone in the northern Gulf of Mexico (Panagopoulos et al., 2014; Kling et al., 2014). The objectives of this specific study are:

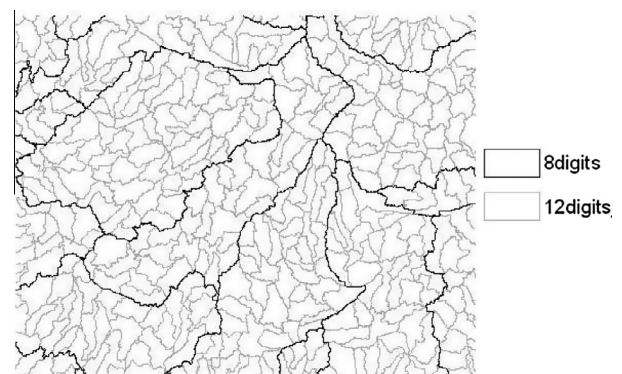


Fig. 1. 8-Digit and 12-digit Hydrologic Unit Codes (HUCs) or watersheds within a small part of the study region within the US Corn Belt.

(a) to demonstrate the first complete effort on the development of the hydrologic and water quality component of this system by presenting an efficient and effective calibration and validation approach, appropriate for large scales, (b) to comprehensively assess the strengths and weaknesses of SWAT to represent current conditions across different parts of the Corn Belt given the 12-digit delineation structure and (c) to share our experiences and provide recommendations to overcome the shortcomings existing in large-scale integrated modeling.

2. Materials and methods

2.1. Watersheds description

The Upper Mississippi River Basin (UMRB) is a headwater basin of the Mississippi River and extends 2100 km from Lake Itasca in Minnesota to just north of Cairo, Illinois, above the confluence with the Ohio River (Srinivasan et al., 2010). It covers approximately 492,000 km² (190,000 mi²), including large parts of Illinois, Iowa, Minnesota, Missouri, and Wisconsin (Fig. 2). The area is referred to as Region 07 at a “2-digit watershed” scale and is further comprised of 131 8-digit watersheds and 5729 12-digit subbasins (USGS, 2012). The average annual UMRB rainfall within the last four decades was 900 mm, ranging from 600 to 1200 mm across

the basin with values generally increasing from west to east. Cropland consists mainly of corn–soybean (C–S) rotations and occupies almost 50% of the total UMRB area, with 75% of the land area characterized by slopes lower than 5%. According to USEPA SAB (2007), 43% of the nitrate load and 26% of the total phosphorus load delivered to the Gulf of Mexico came from the UMRB during 2001–2005, even though the UMRB covers only 15% of the total MARB drainage area. The mean annual flow of the Mississippi River at Grafton, Illinois (Fig. 2) is 3500 m³/s, where the mean annual river loads for N and P have been measured as 500,000 t/y and 30,000 t/y respectively (USGS, 2013). The 70% of the N load appears as NO₃-N.

The OTRB consists of two of the six 2-digit water resource regions that comprise the overall Mississippi River system: Region 05 (Ohio) and Region 06 (Tennessee). The Ohio River starts in Pennsylvania and ends in Illinois, where it flows into the Mississippi River. The Tennessee River joins the Ohio River at Paducah, Kentucky just upstream of the confluence of the Ohio and Mississippi rivers (Fig. 2). The OTRB covers about 528,000 km² (204,000 mi²) and includes a significant portion of seven states as shown in Fig. 2. The region is comprised of 152 8-digit watersheds and 6350 12-digit subwatersheds. The basin receives a high amount of annual rainfall, averaging nearly 1200 mm/y over the last 40 years. The dominant land use in the watershed is forest (50%), cropland (20%) and permanent

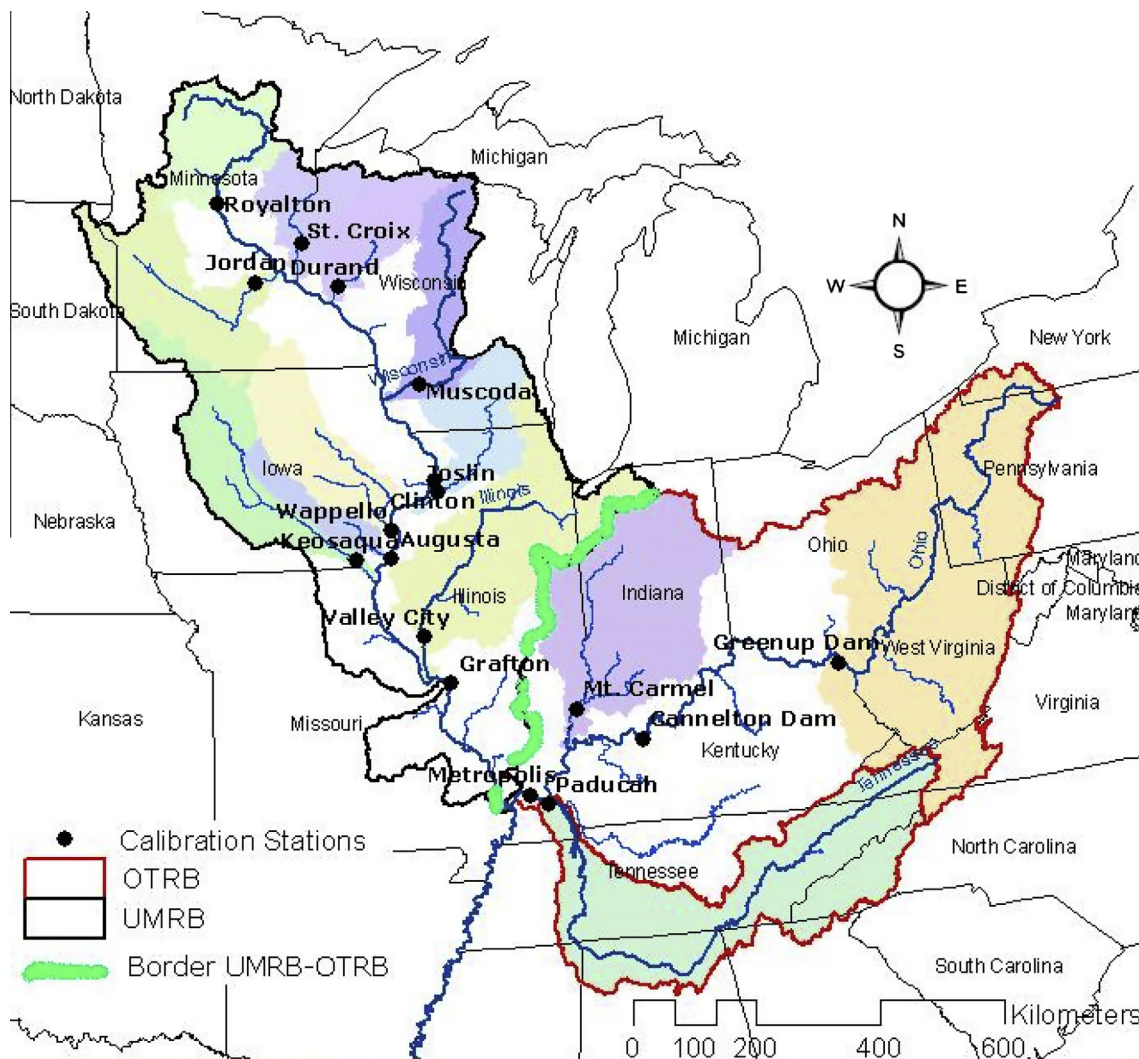


Fig. 2. The locations of the UMRB and OTRB within the US, and the main tributaries, and monitoring site locations, within each study region.

pasture/hay (15%). Corn, soybean and wheat are the major crops grown (Santhi et al., 2014). Compared to the UMRB, the OTRB's slopes are much steeper, especially across much of the forested Tennessee basin, with more than 60% of the total land area characterized by slopes above 5%. The mean annual flow of the OTRB is 8400 m³/s. Similarly to the UMRB, the OTRB contributes 0.5 Gt of N to the downstream Mississippi river on a mean annual basis, with about 65% of this load occurring as NO₃-N. Phosphorus loads have been measured at the most downstream USGS station equal to 48,000 t/y (USGS, 2013).

2.2. SWAT model description

The SWAT model was developed by the US Department of Agriculture in collaboration with Texas A&M University (Williams et al., 2008) and is continuously upgraded with improved versions and interfaces (Arnold et al., 2010; Bosch et al., 2010; Rathjens et al., 2014). A recent release of SWAT version 2012 (SWAT 2012, revision 615) in combination with the ArcGIS (version 10.1) SWAT (ArcSWAT) interface (SWAT, 2013) were used in this study. In SWAT, a watershed is typically delineated into sub-basins and subsequently into hydrologic response units (HRUs), which represent homogeneous combinations of land use, soil types and slope classes in each subbasin. However, a “dominant HRU approach” can also be used in which the dominant land use, soil and slope class within a subbasin are assumed to represent the total subbasin area. In this case, a given subbasin is synonymous with a single HRU, which was the method used in this study to maintain efficiency of this large scale modeling. This decision was however driven by the extent and resolution of available data and justification on why this schematization can be considered appropriate is given next. The physical processes associated with water and sediment movement, crop growth and nutrient cycling are modeled at the HRU scale; runoff and pollutants exported from the different HRUs are routed downstream. Simulation of the hydrology is separated into the land and the routing phase of the hydrological cycle, while sediment yields are estimated with the Modified Universal Soil Loss Equation (MUSLE; Neitsch et al., 2009), which simulates the delivered part of sediment material (and attached nutrients) to the streams accounting for a delivery ratio. SWAT simulates both N and P cycling, which are influenced by specified management practices. Both N and P are divided in the soil into two parts, each associated with organic and inorganic N and P transport and transformations. Agricultural management practices can be simulated with specific dates and by explicitly defining the appropriate management parameters for each HRU. In-field conservation practices such as contour farming, strip-cropping, terraces and residue management are simulated with changes to model parameters that represent cultivation patterns (Arabi et al., 2008). The model is thoroughly described in the SWAT theoretical documentation (Neitsch et al., 2009).

2.3. The auto-calibration SWAT-CUP program and the SUFI-2 algorithm

SWAT-CUP is a software package with a generic interface, where any sensitivity or calibration/uncertainty program can easily be linked to SWAT by manipulating the large number of text files each project consists of (Abbaspour, 2012). SWAT-CUP offers a semi-automatic or combined manual/automatic calibration of SWAT projects, allowing the user to control the initial range of parameter perturbations and seeking to accurately identify their optimum values. Parameters can range either by a percentage from their initial values or within predefined lower and upper bounds. Among the algorithms included in the SWAT-CUP package 2012 (Abbaspour, 2012), the most efficient to calibrate a SWAT project

is the Sequential Uncertainty Fitting (SUFI-2) algorithm (Abbaspour et al., 2007; Yang et al., 2008), the use of which has been found to require fewer simulations to complete a calibration/uncertainty project (Yang et al., 2008). SUFI-2 has been successfully used for regional auto-calibration of very large areas that comprise large portions of entire continents (Pagliero et al., 2014; Schuol et al., 2008a,b) and is highly recommended for the calibration of SWAT models (Arnold et al., 2012).

In SUFI-2, an auto-calibration and uncertainty analysis study starts with large but physically meaningful, user-defined parameter ranges. Parameter uncertainties are decreased iteratively as the algorithm evaluates the performance of the model with updated parameter combinations. The procedure is sequential in nature, meaning that one more iteration can always be made before choosing the final estimates. Thus, the termination of the optimization process provides the best estimate of parameters and also a narrower range of parameter values for possible continuation. The degree to which various uncertainties are accounted for in the simulation is quantified by a measure referred to as the *p*-factor, which is the percentage of measured data (flows, sediments, nutrients) bracketed by the 95% prediction uncertainty (95ppu). This is calculated at the 2.5% and 97.5% levels of the cumulative distribution of an output variable obtained through Latin hypercube sampling, disallowing 5% of the simulations outside this confidence interval. The maximum value for the *p*-factor is 1 (100%), and ideally all measured data should be bracketed, except the outliers. The second measure quantifying the strength of a calibration/uncertainty analysis in SUFI-2 is the *r*-factor, which is the average thickness of the 95ppu band divided by the standard deviation of the measured data. The *r*-factor represents the width of the uncertainty interval or the ‘degree of uncertainty’, which should be as small as possible. Thus, the goal of SUFI-2 is to include the majority of measured data with the smallest possible uncertainty bands. Moreover, as all uncertainties in the conceptual model and inputs are reflected in the measurements (e.g., discharge), bracketing most of the measured data in the prediction 95ppu ensures that all uncertainties are depicted by the parameter uncertainties (Abbaspour, 2012).

2.4. The SWAT UMRB and OTRB parameterization

A SWAT project requires the use of data layers representing land use, soil and topography as well as climate and management information, which, for the study region, are summarized in Table 1. For building the UMRB and OTRB SWAT models, topography was represented by a 30 m digital elevation model (DEM; USGS, 2013) and was used in ArcSWAT to calculate landscape parameters such as slope and slope length. The delineation of the 12-digit watersheds was performed by selecting the predefined ArcSWAT subbasins and streams option, and then inserting the appropriate shape files through the ArcSWAT interface. The area of a 12-digit watershed is typically 4000–16,000 ha (10,000–40,000 ac), compared with around 200,000–400,000 ha (500,000–1,000,000 ac) for an 8-digit watershed. As a result, the total number of subwatersheds is 5729 in the current UMRB modeling structure versus 131 in previous SWAT applications. Similarly, the OTRB has been delineated with 6350 12-digit watersheds relative to the 152 watersheds that would be inserted for a coarser 8-digit schematization.

Historic daily precipitation, maximum temperatures, and minimum temperatures were obtained from the National Climatic Data Center (NCDC-NOAA, 2013) and input to the model from a total of more than 2000 climate stations across the study region. Given the number of 12-digit watersheds used in this study, a climate station is representative for six subbasins on average. Wind speed, relative humidity and solar radiation data, required for estimating potential evapotranspiration using the Penman–Monteith method

Table 1
Summarized information on the data used for the parameterization of the UMRB and OTRB SWAT models.

| Data layer | Description of data layer | Primary data sources |
|------------------------------|--|---|
| Topographic | 30 m digital elevation model (DEM) data used to characterize slopes and slope lengths | USGS (2013) |
| Subbasins | 12-digit Hydrologic Unit Codes (HUCs). 5729 for UMRB, 6350 for OTRB. Area ranging from 40 to 160 km ² | USGS (2012, 2014a) |
| Land use | Assignment of crop rotations or other landuse to each subwatershed; dominant rotations were 2-year sequences of corn and soybean | USDA-NASS (2013) and NLCD (2001) |
| Soil map/layer data | 1:250,000 STATSGO soil map; pertinent soil layer attributes included for each soil type | USDA-NRCS (2013) |
| Daily climate | Daily precipitation and maximum and minimum temperature from around 2000 stations; other meteorological data generated in model | NCDC-NOAA (2013) |
| Subsurface tile drainage | Installed at assumed depth of 1.2 m in poorly drained and relatively flat soils (<2% slope) | Sugg (2007) and Neitsch et al. (2009) |
| Tillage practices | No-till, mulch till, reduced till, and conventional till practices represented as a function of tillage passes and residue cover, and other parameters | Baker (2011) and Neitsch et al. (2009) |
| Other conservation practices | Proxy approach used to represent terraces, contouring, and other practices as a function of slope and slope length | Durancik et al. (2008), USDA-NRCS (2011, 2012), Arabi et al. (2008) and Neitsch et al. (2009) |
| Fertilizer and manure | Nitrogen and phosphorus rates applied in inorganic fertilizer and manure; average rates used for landscapes located within each state | IPNI (2010) |
| Point sources | N and P discharged from thousands of waste treatment plants and other point sources across the two study regions | Maupin and Ivahnenko (2011) and Robertson (personal communication, 2013) |
| Major dams/reservoirs | Key reservoirs on main channels of the Ohio and Mississippi Rivers, and major tributaries – inserted in the model but not simulated at this stage | USACE (2012) |

(which was used in this study), were generated internally in SWAT using monthly climate statistics provided in the ArcSWAT database.

The land use was derived from USDA-NASS Cropland Data Layer (CDL) datasets (USDA-NASS, 2013) in combination with the 2001 National Land Cover Data (NLCD, 2001). This approach included the overlay of CDL datasets in order to create crop rotations used in the region. Specifically, an overlay of multiple years of CDL information has been conducted to produce crop rotation maps with data of 2000–2006, while the NLCD data were used to judge whether a given pixel is cultivated or not. If it was, a crop rotation based on the CDL analysis was assigned, otherwise the non-agricultural NLCD land use type was chosen. The general approach is described in more detail in Srinivasan et al. (2010). From the analysis of the produced maps, it was concluded that two-year corn-soybean (C–S) or soybean-corn (S–C) rotations are dominant within the overall agricultural land portion of the region (>70%) with a smaller fraction managed with continuous corn (C–C) rotation and much smaller fractions with other multi-year rotations including other crops. The distinction between C–S and S–C rotations is very important for the simulation since we need to ensure that both corn and soybean are produced every calendar year in the Corn Belt, while specific management practices associated to each one of the crops (e.g. high nitrogen fertilization of corn) are applied to an appropriate extent across the study area in each simulation year. Moreover, to consider the relatively recent crop rotation schemes (2000–2006) representative for the past years (back to 1975) and the most recent ones (2007–2010) we had to rely on the fact that, traditionally, the rotations in the area were the ones selected from the recent available data and that changes were not important in the last decades.

Soil characteristics were represented by the USDA 1:250,000 STATSGO soil data (USDA-NRCS, 2013) with approximately 600 and 1000 soil types lying within the UMRB and OTRB, respectively. The study area was then divided into three slope classes: (a) <2%, (b) 2–5%, and (c) >5% based on the needs to assign tiles to flat areas (<2%) and differentiate the reduction of the management factor (USLE_P) to represent the extent of existing conservation practices (described next). Then, we overlaid land use and soils on each of the 5729 UMRB subbasins and 6350 OTRB subbasins in ArcSWAT to determine the dominant land use type, soil and slope class in each subbasin. This choice was essential for keeping the size of

the model at a practical limit; however, the accuracy achieved here is significantly higher compared to several similar large-scale applications which used the dominant HRU approach in larger subbasins (e.g., Pagliero et al., 2014; Rossi et al., 2009; Schuol et al., 2008a,b). With the dominant HRU approach in this study we take advantage of the refined 12-digit watershed schematization to capture land use, soil and slope information to a high extent by keeping the number of HRUs at the lowest possible level and maximizing the computation efficiency.

The majority of the STATSGO soil types (80%) remained in both basins following the HRU delineation. Likewise, slope distribution within both basins remained very close to the original distribution, with 75% of the UMRB area defined by slopes <5% and the majority of OTRB slopes >5%, except for agricultural land in the northwestern part of the region. However, SWAT calculates a single average slope for each subbasin of a watershed project, which is included in all subsequent calculations. This, although not ideal, is definitely more representative than calculating slopes for a larger watershed (an 8-digit for example) and corresponding them to all HRUs within it. It should also be noted that in a possible 8-digit model with multiple HRUs in each subbasin we would have applied a 5–15% threshold for land use, soil and slopes to force the model to ignore the types of low percentage. Considering that an 8-digit contains on average 40–50 12-digits it is obvious that the 8-digit option with the thresholds should have resulted in more than 40–50 different combinations of land/soil/slope in order to disturb the original percentages less than the '12-digit and dominant HRU' option. Moreover, the dominant approach resulted in slight increases of total cropland from 46% to 47% and 18% to 19% in the UMRB and OTRB, respectively, with UMRB cropland concentrated across a 230,000 km² area of Minnesota, Iowa and Illinois versus a 100,000 km² OTRB area mainly in Illinois, Indiana and western Ohio. Despite the preservation of the total cropland, minor rotations such as corn-corn-soybean or corn-soybean-wheat, which occupied less than 5% of the total cropland area in most of the 12-digit subbasins, were eliminated in this process and were replaced by the dominant rotation types of C–S, S–C and C–C. The 3-year rotations were however minor, while they always included the two dominant crops in the region. Therefore, simulation results are practically not influenced by replacing 3-year rotations by the typical 2-year rotations in a very small part of the study area. Forest land also increased, while the fractions of

the basins occupied by pasture/hay and urban areas decreased slightly relative to the original map. Overall, the land use distribution within the dominant HRU models was not deviated significantly from the original, while the total cropland area in the Corn Belt, which is of particular interest for pollutant load simulation in this study, remained practically unchanged.

Subsurface tile drain systems have been installed in Corn Belt region subareas that are dominated by poorly drained soils and have been documented to be key conduits of nitrate from cropland landscapes to stream systems (David et al., 2010). Detailed maps of tile drain locations do not exist for most of these subareas. However, Sugg (2007) estimated the extent of tile drained soils at the county level for the entire US. Thus, these county-level estimates were first aggregated to the 8-digit watershed level to establish the same spatial reference with available fertilizer and tillage data (described below). The tile drains were then assigned to 12-digit watersheds within a given 8-digit watershed that were characterized by: (1) cropland land use, slopes <2%, and with poorly drained soils (hydrologic groups D or C), or (2) cropland, slopes <2%, and hydrologic group B soils. The group B assignments were performed only if needed to meet the total tile drained area within an 8-digit watershed. All tile drains were simulated with the following assumptions, typical in SWAT studies for the area (e.g. Schilling and Wolter, 2009): a depth of 1200 mm, the time to drain a soil to field capacity (24 h), and the amount of time required to release water from a drain tile to a stream reach (72 h), which are the SWAT DDRAIN, TDRAIN, and GDRAIN input parameters, respectively (Neitsch et al., 2009).

Spatial representation of tillage types (conventional, reduced, mulch, and no-till) were incorporated in the modeling system based on estimates of the distributions of different tillage types at the 8-digit watershed level (Baker, 2011). We assumed that the most recent data of 2004 were the most representative to our work. These 8-digit% data of each tillage type were disaggregated to the 12-digit subbasin level, within a given 8-digit watershed, in a manner that maintained the same overall distribution of tillage types as reported at the 8-digit watershed level, to the extent possible. Each tillage type was represented by two tillage passes (and corresponding levels of crop residue incorporation: 5–95% mixing efficiency and 25–150 cm tillage depth (with lower values corresponding to no-till), as well as appropriate values of Manning's roughness coefficient for overland flow (OV_N), which ranged between 0.14 and 0.20 (higher values for no-till) and crop cover factor (USLE_C), which is used in the MUSLE erosion estimations (Neitsch et al., 2009). Specifically, the default USLE_C factor (0.2) for corn and soybean in the SWAT database was used for conventional tillage and this value was lowered gradually to represent reduced (0.15) and conservation tillage types (mulch (0.10), no-till (0.05)). Based on the tillage data used, almost two-thirds of the crop land in both UMRB and OTRB is treated with conservation tillage. In the typical C–S rotation simulated in this study, the two tillage passes of each tillage type are taking place in April and are followed by corn sowing and fertilization (information is given next) in May with a crop harvest operation in October. The alternate rotation year begins again with the tillage passes, continues with soybean sowing in April, P fertilization and ends with the harvest of the crop in October.

Regional estimates of the distribution of other conservation practices are not currently publicly available. To address this deficiency we used a proxy approach that was based on information provided in the Conservation Effects Assessment Project (CEAP; Duriancik et al., 2008) UMRB (USDA-NRCS, 2012), and OTRB (USDA-NRCS, 2011) studies. These studies report that a significant part of the cropland in the UMRB and OTRB has at least one in-field conservation practice (terrace, strip-cropping, contouring), while highly erodible land is managed to a much greater extent compared to less erodible areas. In our model the in-field conservation

practices are likely to be present in all the HRUs due to their relatively large areas (12-digit subbasins), which aggregate a large number of farm-fields. Therefore, we simulated the effect of in-field conservation practices on erosion control in all of them by reducing the management (P) factor of the MUSLE (Neitsch et al., 2009), which is the major parameter that governs the representation of all such practices in the model (Arabi et al., 2008). The P factor was reduced from the default value of 1.0 (no management) to values 0.2–0.4 in all of the agricultural 12-digit subbasins (HRUs) of the basins, followed by appropriate modifications on the slope length (Arabi et al., 2008). We specified higher reductions of the P factor in high-sloping agricultural HRUs and slighter reductions in low sloping ones to address the possible increased level of management in highly erodible land. Curve number (CN) adjustments, which can also be used to represent in-field conservation practice effects (Arabi et al., 2008), were performed during the hydrologic calibrations (described below); the reduced CN values likely reflect the expanded adoption of conservation tillage across the Corn Belt region (USDA-NRCS, 2011, 2012). Land managed with long-term conserving cover, such as Conservation Reserve Program (CRP), is represented indirectly in the models as pasture, hay land or other grassland.

Fertilizer (including recoverable manure) application rates were calculated based on recent (2007) fertilizer N and P mass estimates at the 8-digit level obtained from the Nutrient Use Geographic Information System (NuGIS) for the US. (IPNI, 2010). Specifically, we divided these 8-digit mass data by the crop areas to calculate the fertilization rates (kg/ha) needed by SWAT. However, we encountered unreasonable values for a large number of 8-digit units, which were mostly attributed to uncertainties of the fertilizer sales data used in NuGIS and their correspondence with the area of their actual usage. Thus a simplified approach was used based on statewide averages from the NuGIS data (aggregation of all 8-digit mass information within a state and division with the crop areas of the state), which resulted in very reasonable annual average N and P rates applied to C–S and S–C rotations that ranged between 117–156 and 25–34 kg/ha, respectively, with N applied only to corn. In C–C rotations, the applied N was increased by 50 kg/ha compared to the C–S rotation of a given state, based on typical rates used for the two different rotations as reported by Sawyer (2012). For hay and pastureland we used the auto-fertilization routine of SWAT by setting a 70 kg N/ha/y maximum limit of application to roughly account for the unrecoverable manure reported in NuGIS for each state (IPNI, 2010).

Loads of mineral N and P released directly to the streams and rivers of UMRB and OTRB were also inserted to the model from thousands of point sources across the region (Maupin and Ivahnenko, 2011; Robertson, D. Personal Communication. U.S. Geological Survey, Lacrosse, WI). Specifically, we obtained annual effluent data for the years 1992, 1997 and 2002 for almost 15,000 installations along with their locations across the study area and we aggregated these loads per 12-digit subbasin. According to the most recent data of 2002, the annual point source contribution in UMRB was 82,000 t N and 7000 t P, while total point source loads in the OTRB were 87,000 t N and 5500 t P. These point sources were simulated as constant daily mineral N or P loads for the appropriate 12-digit subbasins.

Finally, reservoir data in the basins were obtained from the national inventory of dams (USACE, 2012), including information for the surface area and the normal and maximum storage, which is relevant to SWAT. No operation details were available with information on release rates and timings. From the thousands of large, small and very small reservoirs included in the data only 50 were inserted to the UMRB and OTRB models to skip existing ArcSWAT limitations when their number becomes very high. This number would be however adequate to reproduce the potential

reservoir influence on water flow and pollutant transport along rivers as they were the largest ones and represented the vast majority of total artificial lake volume in the study area. However, no reservoir operation was finally modeled in this project due to high uncertainties in their simulation. Specifically, we encountered severe problems in simulating pollutants when we used either the default or adjusted values for the parameters governing sediment and nutrient settling in the reservoirs. SWAT was consistently simulating unreasonable sediment and nutrient exports from the reservoirs disturbing their flow in a way that by no means is expected in nature. Sediment and nutrient fluxes were either negligible downstream a reservoir or dramatically increased due to an unexpected supply from the reservoir itself (resuspension). Reservoirs operation was thus deactivated by simply defining a starting operation date at the end of the simulation period.

2.5. Streamflow calibration approach

SWAT was calibrated using monthly streamflow data (1975–2010) obtained for 12 UMRB and 5 OTRB USGS stations (Fig. 2; USGS, 2013). To accelerate the auto-calibration process with the use of SWAT-CUP and SUFI-2, we used only the most recent 14-year period for calibration and the older data for validation. We calibrated the majority (13) of the subregions simultaneously because they are “hydrologically independent” (Fig. 2 and Table 2). The only exceptions were Clinton and Grafton in the UMRB and Cannelton Dam and Metropolis in the OTRB, which receive flows and pollutants from upstream river basins. Each of the 13 ‘hydrologically independent’ subregions corresponds to either the most upstream part of the main stem (Royalton for Mississippi River or Greenup Dam for Ohio River) or a major tributary flowing into them (i.e., the Minnesota, Iowa, Skunk, Des Moines, St. Croix, Wisconsin, Chippewa, Illinois, and Rock Rivers in UMRB and the Wabash and Tennessee Rivers in OTRB). The closest 12-digit subwatershed outlet was used to represent the location of each of the major subregions (Fig. 2). This approach resulted in only minor inaccuracies due to the density of the UMRB and OTRB 12-digit subwatersheds. Table 2 summarizes the information related to the monitoring points.

Each parameterized subregion was manipulated separately by the SWAT-CUP interface for streamflow auto-calibration and uncertainty analysis with SUFI-2. After a manual experimentation with SWAT parameters in the region and a literature review

(Arabi et al., 2008; Lenhart et al., 2002; Van Griensven et al., 2006), this study used eight sensitive parameters (Neitsch et al., 2009): five related to groundwater (ALPHA_BF, GW_DELAY, GWQMN, RCHRG_DP, and GW_REVAP), the curve number (CN2), the soil evaporation compensation coefficient (ESCO) and the available soil water capacity of the first soil layer (SOL_AWC(1)), in order to calibrate the 13 hydrologically independent individual watersheds within 500 simulations (auto-calibration termination criterion). Prior to that we had adjusted the three of the five snow parameters in the ‘bsn’ file of SWAT by checking snowmelt magnitude and hydrograph shapes in a first series of manual SWAT runs. Both the melt factors SMFMX and SMFMN (Neitsch et al., 2009) were modified to 1 mm H₂O/°C day, while the snow pack temperature lag factor (parameter TIMP – Neitsch et al., 2009) was set to 0.4. These parameters were not further adjusted within the automatic process since they could not be adjusted at the HRU scale as all others but only at the entire basin scale. The CN and SOL_AWC(1) were the only parameters allowed to alter by a percentage from the default values ($\pm 20\%$), while all others were modified with absolute values within realistic ranges. The best estimate of parameters for each subregion was next adapted as the calibrated parameter-set to calibrate the same eight parameters of the intermediate watersheds. Calibration on the two sites of each basin was conducted consecutively. This was done by allowing SUFI-2 to change the parameters only in the 12-digit subbasins that corresponded to these intermediate areas (see Table 2). In all processes, the SUFI-2 optimization algorithm was seeking to identify the optimum parameters by using the Nash–Sutcliffe modeling efficiency (NS; Moriasi et al., 2007; Krause et al., 2005) as the objective function. However, the results of the auto-calibration were also evaluated according to the percent bias (PBIAS; Moriasi et al., 2007) and the coefficient of determination (R^2) (see Krause et al., 2005 for more detailed description) as well as the SUFI-2 p and r uncertainty factors. Satisfactory NS and PBIAS monthly results were evaluated per criteria suggested by Moriasi et al. (2007); i.e., NS values ≥ 0.50 and PBIAS values $\leq \pm 25\%$. Graphical comparisons between the simulated and measured streamflow values were also conducted.

2.6. Sediment and nutrient calibration approach

In-stream sediment, nitrate-N (NO₃-N), organic N, and organic and mineral P data were available for some of the stations of

Table 2
The gauge sites used for streamflow calibration with SUFI-2 in this study with their official USGS reported upstream area as well as their total drainage and calibrated area in SWAT (see also Fig. 2).

| Gauge site (Fig. 2) | River | River basin | State | USGS station | Hydrologically independent? ^a | Calibrated area (km ²) | Total upstream drainage area (km ²) |
|---------------------|-------------|-------------|-------|--------------|--|------------------------------------|---|
| Royalton | Mississippi | UMRB | MN | 05267000 | Yes | 29,970 | 29,970 |
| Jordan | Minnesota | UMRB | MN | 05330000 | Yes | 43,280 | 43,280 |
| St. Croix Falls | St. Croix | UMRB | WI | 05340500 | Yes | 16,250 | 16,250 |
| Durand | Chippewa | UMRB | WI | 05369500 | Yes | 24,140 | 24,140 |
| Muscoda | Wisconsin | UMRB | WI | 05407000 | Yes | 27,290 | 27,290 |
| Wappelo | Iowa | UMRB | IA | 05465500 | Yes | 32,710 | 32,710 |
| Augusta | Skunk | UMRB | IA | 05474000 | Yes | 11,270 | 11,270 |
| Keosauqua | Des Moines | UMRB | IA | 05490500 | Yes | 36,530 | 36,530 |
| Joslin | Rock | UMRB | IL | 05446500 | Yes | 24,550 | 24,550 |
| Valley City | Illinois | UMRB | IL | 05586100 | Yes | 69,540 | 69,540 |
| Clinton | Mississippi | UMRB | IA | 05420500 | No | 75,230 | 222,500 |
| Grafton | Mississippi | UMRB | IL | 05587450 | No | 50,600 | 447,700 |
| Greenup | Ohio | OTRB | KY | 03216600 | Yes | 159,600 | 159,600 |
| Paducah | Tennessee | OTRB | KY | 03609500 | Yes | 104,200 | 104,200 |
| Mt. Carmel | Wabash | OTRB | IL | 03377500 | Yes | 74,810 | 74,810 |
| Cannelton Dam | Ohio | OTRB | IN | 03303280 | No | 90,400 | 250,000 |
| Metropolis | Ohio | OTRB | IL | 03611500 | No | 97,290 | 526,300 |

^a Yes indicates that the respective system is hydrologically independent. No indicates gauge sites that receive water from upstream calibrated watersheds; the calibrated area in these SUFI-2 projects is the intermediate area between the gauge site listed in the first column and the preceding upstream gauge site (see Fig. 2).

Table 2 on a monthly basis for similar or shorter time-periods than the streamflow calibration/validation period (1975–2010). All observed data were obtained from the USGS (2013) and were provided as complete monthly time-series. Sediment data was available only for a subset of UMRB gauge sites, primarily at the outlets of large watersheds as well as along the Mississippi river. The USGS monthly time-series of nutrient constituents were developed with the use of LOADEST (Runkel et al., 2004; USGS, 2014b). The water quality observations reflect increased uncertainty compared to hydrologic observations, in part due to increased inherent uncertainty in the river basin processes of pollutant transport. Moreover, SWAT is restrictive in that a large number of sediment and nutrient-related parameters can only be adjusted at the entire basin scale, not allowing much heterogeneity. Thus a manual calibration approach was considered more appropriate for performing the nutrient and sediment calibration.

The pollutant calibration process consisted of ensuring that key upland sediment and nutrient processes as well as point sources were accounted for and that the predictions at the monitoring stations were acceptable. Specifically, our goal was to calibrate the predicted average annual loads within a minimum percent bias or prediction difference from the observed data. According to Moriassi et al. (2007), monthly model simulations can be judged as satisfactory if PBIAS is measured up to $\pm 55\%$ for sediment and $\pm 70\%$ for N and P. However, to ensure a more realistic simulation we selected more strict limits with $\leq 30\%$ bias for sediment and $\leq 40\%$ bias for nutrients (Santhi et al., 2014). The NS efficiency and R^2 were also calculated, although they were not used as the critical indices for the calibration success here as explained next in the text.

Simulation of UMRB and OTRB upland erosion was partially addressed by the previously described tillage and conservation practice related parameterizations including adjustments in the P factor and slope lengths and was considered a viable option to keep spatial heterogeneity of sediment source across the basin. The peak rate adjustment factor (ADJ_PKR) for sediment routing in the sub-basins was also reduced to 0.5 from the default value of 1.0 in both river basins as a final calibration step, which can only be adjusted at the overall basin level and impacts the amount of erosion generated in HRUs (Neitsch et al., 2009). Channel erosion parameters can also be adjusted in SWAT including the peak rate adjustment factor for sediment routing in the main channel (PRF) and the linear (SPCON) and exponential (SPEXP) coefficients for sediment that can be re-entrained during channel sediment routing. The parameters can assist in simulating the contribution of the main channel to the total sediment river load by considering sediment deposition and channel degradation, in an attempt to capture phenomena such as stream bank erosion which is an important sediment source in many river basins in the Corn Belt region (Belmont et al., 2011; Schilling et al., 2011). However, quantifying these processes is difficult due to the high level of uncertainty and the fact that the SWAT channel erosion parameters can only be adjusted at the overall basin level. Thus adjustment of these parameters was considered unrealistic for these applications. Thus, upland erosion was considered dominant in this study compared with the channel erosion, which at least for the OTRB is in agreement with the study of Santhi et al. (2014).

Additional adjustments were made to parameters related to the N and P cycles to perform the nutrient calibrations. The N percolation coefficient (NPERCO) and the CDN and SDNCO parameters, which govern denitrification from soil (Neitsch et al., 2009), were adjusted to perform the $\text{NO}_3\text{-N}$ calibration. NPERCO governs the amount of $\text{NO}_3\text{-N}$ removed from the surface soil layer via runoff versus removal through percolation, and was set at 0.6 and 0.5 for the UMRB and OTRB, respectively. Denitrification is also a very uncertain watershed process, whose magnitude cannot be easily

defined. We slightly altered the denitrification exponential rate coefficient CDN (to 0.1 in both basins) and the denitrification threshold water content SDNCO (to 1.0 in UMRB and to 0.99 in OTRB) in order to simulate a reasonable denitrification rate, expected within a 10–20% of the annual N fertilization rate in crop areas (Neitsch et al., 2009) and within the range 3.8–21 kg/ha/y reported by David et al. (2009).

On the other hand, the nutrient parameters included in the bsn file of SWAT were not adequate to capture organic N and P forms which are strongly correlated with sediment loads. Thus, following sediment calibration, the TN and TP loads in several stations remained moderately and considerably overestimated (almost double) compared to the observations, respectively, for both simulated regions. Adjustment of the P percolation coefficient (PPERCO), the P soil partitioning coefficient (PHOSKD), and the P availability index (PSP) did not result in significant TP prediction improvements, because these parameters mainly affect soluble P loss estimates which were a minor component of the overall estimated TP losses in both basins. Thus, we then examined the initial levels of soil N and P (parameters SOL_ORGN(1) and SOL_ORGP(1)) in the top cropland soil layers which are typically estimated internally in SWAT as a function of soil carbon (Neitsch et al., 2009). The relatively soil high carbon contents in the study areas (especially the UMRB) resulted in initial soil N and P levels that were often unrealistic with organic N and P amounts; i.e., >5000 ppm and 600 ppm for some soils, respectively. This problem, coupled with the fact that the high soil N and P levels affected the SWAT simulations for long durations (well beyond the initial model warm-up periods) revealed that relying on the SWAT default values for soil organic N and P was not a viable option. Therefore, these soil parameters were manually defined for different parts of the UMRB and OTRB basins to enhance N and P calibration. We applied a percentage reduction to all the HRUs (12-digit subbasins) located above the same calibration point to maintain heterogeneity.

Finally, in-stream nutrient processes were not simulated in this study because such processes are highly uncertain and can only be simulated in SWAT at the entire basin level, thus ignoring varying conditions across different order streams and between different subregions. In addition, there is evidence that the magnitude of several such processes is not important at large scales. For example, denitrification in water (streams, rivers), is considered negligible in the UMRB and OTRB due to the fast $\text{NO}_3\text{-N}$ transport from field-level tile-drainage systems to higher order streams (major tributaries and main channels) within a few days to weeks in the winter and spring (David et al., 2009).

3. Results and discussion

3.1. Hydrologic performance of the Corn Belt SWAT models

Table 3 summarizes the final hydrologic parameter values that resulted from the auto-calibration with SUFI-2 for all 17 gauge sites in UMRB and OTRB. The results clearly show that curve numbers (CN2) were reduced in almost all of the UMRB and OTRB sub-basins, with the greatest reductions occurring within the UMRB. These results indicate a possible overestimation of the default CN values in SWAT. On the other hand, ESCO was predicted within a narrow range around the default value of 0.95, thus the SWAT initial value could be considered as an acceptable value for the entire Corn Belt region and its exclusion from the calibration would possibly not alter hydrologic predictions considerably. The SOL_AWC(1) does not present a standard behavior with changes from the default values ranging greatly between different subregions. This could indicate that the coarse STATSGO soils lack accuracy which could be potentially mitigated with more detailed soil

Table 3
SUFI-2 best estimates of hydrologic parameters in different areas of UMRB and OTRB.

| Calibration point (Fig. 2) | GW_DELAY | ALPHA_BF | GWQMN | GW_REVAP | RCHRG_DP | CN2 | ESCO | SOL_AWC(1) |
|----------------------------|----------|----------|-------|----------|----------|-------|-------|------------|
| Allowable range | 0–300 | 0–1 | 0–300 | 0–0.2 | 0–0.5 | ±0.2 | 0.7–1 | ±0.2 |
| Royalton | 169 | 0.09 | 25 | 0.01 | 0.27 | –0.13 | 0.98 | –0.05 |
| Jordan | 28 | 0.63 | 0.7 | 0.02 | 0.01 | –0.13 | 0.94 | –0.10 |
| St. Croix Falls | 27 | 0.79 | 55 | 0.02 | 0.33 | –0.16 | 0.96 | –0.06 |
| Durand | 259 | 0.54 | 50 | 0.02 | 0.21 | –0.17 | 0.83 | –0.05 |
| Muscoda | 323 | 0.53 | 14 | 0.03 | 0.15 | –0.12 | 0.94 | 0.18 |
| Wapello | 114 | 0.63 | 118 | 0.03 | 0.07 | –0.12 | 0.95 | –0.18 |
| Augusta | 39 | 0.48 | 15 | 0.02 | 0.21 | 0.02 | 0.97 | –0.10 |
| Keosauqua | 86 | 0.49 | 204 | 0.04 | 0.05 | –0.17 | 0.90 | 0.18 |
| Joslin | 180 | 0.85 | 188 | 0.01 | 0.08 | –0.13 | 0.92 | –0.15 |
| Valley City | 49 | 0.65 | 56 | 0.02 | 0.04 | –0.14 | 0.95 | –0.20 |
| Clinton ^a | 68 | 0.42 | 61 | 0.02 | 0.02 | –0.15 | 0.89 | 0.04 |
| Grafton ^a | 169 | 0.64 | 5.3 | 0.00 | 0.05 | –0.20 | 0.97 | 0.02 |
| Greenup | 16 | 0.51 | 161 | 0.02 | 0.02 | –0.07 | 0.89 | 0.09 |
| Paducah | 6.2 | 0.17 | 119 | 0.18 | 0.24 | –0.17 | 0.83 | 0.07 |
| Mt. Carmel | 33 | 0.58 | 20 | 0.07 | 0.10 | –0.19 | 0.93 | –0.14 |
| Cannelton Dam ^a | 13.5 | 0.14 | 60 | 0.03 | 0.02 | –0.09 | 0.91 | –0.05 |
| Metropolis ^a | 58.5 | 0.75 | 155 | 0.05 | 0.03 | 0.01 | 0.99 | 0.05 |

^a These calibration points receive water from upstream calibrated watersheds and their SUFI-2 calibration was done after the termination of the auto-calibration of the upstream areas. For CN2 and SOL_AWC(1), both allowable ranges and best estimates express the change from the default value as a fraction, for example, –0.13 corresponds to 13% reduction and the allowable change of the parameters was within –20% and 20% of the default values.

Table 4
Monthly streamflow calibration and uncertainty analysis statistics for UMRB and OTRB subregions.

| Calibration point (Fig. 2) | Calibration (1997–2010) | | | | | Validation (1975–1996) | | |
|----------------------------|-------------------------|----------|-----------------------|------|--------|------------------------|------|--------|
| | <i>p</i> | <i>r</i> | <i>R</i> ² | NS | PBIAS | <i>R</i> ² | NS | PBIAS |
| Royalton | 0.67 | 1.44 | 0.48 | 0.46 | 7.43 | 0.47 | 0.44 | 13.19 |
| Jordan | 0.51 | 0.72 | 0.79 | 0.75 | 21.16 | 0.85 | 0.81 | 9.45 |
| St. Croix Falls | 0.65 | 1.13 | 0.81 | 0.67 | 23.16 | 0.72 | 0.57 | 25.32 |
| Durand | 0.77 | 1.24 | 0.71 | 0.69 | 11.51 | 0.54 | 0.44 | 19.96 |
| Muscoda | 0.76 | 1.81 | 0.64 | 0.61 | 2.70 | 0.53 | 0.49 | 11.92 |
| Wapello | 0.43 | 0.66 | 0.77 | 0.75 | 5.76 | 0.82 | 0.81 | 0.11 |
| Augusta | 0.57 | 0.56 | 0.90 | 0.90 | 2.88 | 0.90 | 0.90 | –1.18 |
| Keosauqua | 0.54 | 0.62 | 0.67 | 0.62 | 20.56 | 0.71 | 0.66 | 17.44 |
| Joslin | 0.38 | 1.04 | 0.69 | 0.59 | 4.38 | 0.62 | 0.55 | 0.59 |
| Valley City | 0.48 | 0.76 | 0.66 | 0.50 | –12.17 | 0.70 | 0.43 | –18.02 |
| Clinton ^a | 0.43 | 0.50 | 0.66 | 0.55 | 10.41 | 0.70 | 0.65 | 10.80 |
| Grafton ^a | 0.33 | 0.17 | 0.72 | 0.69 | 2.92 | 0.74 | 0.72 | 1.37 |
| Greenup | 0.71 | 0.80 | 0.90 | 0.89 | –5.25 | 0.87 | 0.87 | 3.40 |
| Paducah | 0.85 | 1.05 | 0.82 | 0.77 | 12.74 | 0.86 | 0.71 | 27.17 |
| Mt. Carmel | 0.77 | 0.89 | 0.83 | 0.82 | –3.47 | 0.74 | 0.68 | –1.48 |
| Cannelton Dam ^a | 0.52 | 0.30 | 0.92 | 0.92 | –1.38 | 0.89 | 0.89 | 2.14 |
| Metropolis ^a | 0.44 | 0.18 | 0.90 | 0.89 | 6.87 | 0.88 | 0.83 | 14.42 |

Each calibration point was selected as the outlet of the 12-digit subwatershed located closer to the existing USGS flow observation station and its exact location is shown in Fig. 2. The name of each large upstream area is defined from the homonymous river. In the first two columns with numerical results, *p* and *r* are the percentage of observed data bracketed by the 95% ppv and the degree of uncertainty respectively, *R*² is the coefficient of determination, NS the Nash–Sutcliffe efficiency and PBIAS the percent bias with positive values indicating model underestimations and negative overestimations (Moriasi et al., 2007).

^a These calibration points receive water from upstream calibrated watersheds and their SUFI-2 calibration was done after the termination of the auto-calibration of the upstream areas.

data. Finally, the five groundwater parameters received such values that optimized groundwater contribution to streamflow in a way that simulated streamflows are improved toward the observed. Among the major findings here is that groundwater revap is negligible in most subregions receiving values close to the minimum default value of the range implying that GW_REVAP could be excluded from the calibration. Also, in most of the forested subregions of the study area there is a considerable fraction of percolated water which is further percolated to the deep aquifer and lost from the system (parameter RCHRG_DP > 0.20),

indicating that possible hydrologic/hydrogeologic particularities exist in these areas.

Table 4 presents the statistical results for comparisons of the aggregated monthly SWAT simulated streamflows versus corresponding measured streamflows. The results indicate a high *p* factor, acceptable *r* factor and *R*² values, and satisfactory monthly NS values (>0.5 per the criteria suggested by Moriasi et al., 2007) for most of the 17 calibrated areas within the UMRB and OTRB. However, calibration and/or validation NS values were <0.5 for three UMRB subregions: Royalton, Durand, and Muscoda (see Fig. 2). Weaknesses were also reflected in the other statistics calculated for these three regions. This was likely due to the impact of natural lakes and/or wetlands on hydrology in these areas, which can attenuate peak flows and maintain considerable flows in low-flow periods, a situation that could not be well captured by the current wetlands parameterization.

Virtually all of the PBIAS results (Table 4) are acceptable per the criterion of <25% deviation suggested by Moriasi (2007). The underestimation of runoff in the majority of subregions (positive PBIAS) reveals the general tendency of SWAT to satisfy ET requirements in advance of runoff simulation. This situation is highlighted for example, by the Minnesota River basin (Jordan in Table 4) and St. Croix results, where the calibration PBIAS were the highest of all the simulated basins. The lowest precipitation occurs in the Northern subregion of the UMRB and the ET requirements in some months highly exceeded water availability, resulting in low runoff simulation in SWAT. Overall, the validation statistics support the quality of calibration and in many cases were even better.

The results of Table 4 also indicate that for the greatest part of the two basins SUFI-2 narrowed the uncertainties to acceptable levels. The *p* factor is greater than 0.5 for the majority of the calibration points, showing that more than 50% of the observed data are bracketed by the 95ppv. This is considered highly acceptable for the large scale of this application and is supported from the low *r* values, which were always close to the desirable limit of unity or lower than that. However, exceptions of the rule are the *r* statistics calculated for the three northern UMRB subregions (Royalton, Durand and Muscoda), where the algorithm captured most of the observed data but with a relatively increased degree of uncertainty (high *r* values). It should also be noted that for all four gauge sites that were not independently calibrated (indicated with an asterisk in Table 4), the *p* and *r* factors were always low. Actually, flow in these areas is to a great extent predefined from

the already calibrated upstream areas, leaving a small degree of freedom for SUFI-2 to affect total flows in these areas. Therefore, the r factor was extremely low demonstrating a very small width of the 95ppu band, which inevitably occurred in an expense of the p factor. The relatively low p factor values in these areas indicate that the 95ppu at these points did not capture the majority of observations. However, the fact that the SUFI-2 calibration of these sites is not independent from other sites (head watersheds already calibrated) and is based on parameter adjustments within only part of the total upstream area reduces the reliability of these statistics for judging the calibration effectiveness. The calibrated statistics at these sites are influenced significantly from the large upstream areas which have been already calibrated. Besides, the success of the process in the upstream areas automatically leads to good predictions at the most downstream locations, with NS, R^2 and PBIAS strongly supporting this finding, especially in the OTRB (Cannelton Dam and Metropolis).

Fig. 3 shows the graphs of simulated versus observed monthly flow data for the entire simulation period including both the most recent years used for calibration (1997–2010) and those used for validating model performance (1975–1996). The graphs demonstrate strong agreement between simulated and observed monthly flows across the study region. In particular, both peaks and recession limbs are well predicted at the majority of the gauge sites within the region, especially for the OTRB. In UMRB, there are successful graph predictions with respect to both peaks and recessions in all the five major agricultural subregions namely: Iowa, Des Moines, Skunk, Rock and Illinois river basins that is of utmost importance for capturing the intra-annual variability of non-point source pollutant load transported to the outlet. On the other hand, results are poorer for the northern forested subregions of Royalton, St. Croix, Wisconsin and Chippewa, primarily for the reasons stated previously. However, as crop areas in these subregions are small their influence on pollutant transport downstream is minor and thus the results do not greatly impact water quality predictions for the UMRB. For example, nutrient measurements in St. Croix show that mean annual $\text{NO}_3\text{-N}$ and TP loads of this subregion represent the 0.3% and 0.8% of the measured loads at Grafton respectively.

3.2. Water quality performance of the Corn Belt SWAT models

Table 5 summarizes the mean annual simulated and observed sediment, TN and TP for the entire simulation period, following manual calibration of both models. Due to the lack of sediment observation in the OTRB we report the mean annual observed value given in Santhi et al. (2014) for the Mt. Carmell and Metropolis stations and use it for comparison with our simulations. Moreover, Table 5 includes the lower and upper intervals (95% confidence limits) of the annual nutrient measurements calculated and provided by USGS (2013). Thus, apart from giving the level of annual predictions at several gauge sites, the table provides an additional measure of model performance for nutrients, which is considered successful when the simulated value lies within the observed confidence range. Unfortunately, neither the USGS, nor Santhi et al. (2014) provide lower and upper sediment limits for the stations of Table 5. As can be clearly observed, the SWAT annual predictions are acceptable for almost all of the stations and pollutant types.

Table 6 summarizes the monthly statistics produced from sediment and nutrient calibration in the study region. The first goal for these large-scale applications is more to ensure that the predictions replicate observations within an acceptable range rather than to produce a perfect monthly multi-year reproduction. Therefore, PBIAS is considered the primary index to judge the model's

performance here, although both the NS and R^2 statistics were also evaluated.

Monthly sediment time-series were available for only four sites in UMRB and for a limited number of years, which did not allow the use of any data for validation. For the particular case of sediments in OTRB, statistics could not be calculated due to lack of monthly observed data. However, before moving to nutrient calibration in OTRB, we compared the average annual SWAT sediment predictions with the respective reported observations (Santhi et al., 2014) to assess the accuracy of the magnitude of the sediment estimates (see Table 5 and associated discussion). The PBIAS index in Table 6 shows that sediment predictions in the UMRB are always within the range of observations as evidenced by the low bias results. The calibration success is strengthened by the NS efficiency which was positive in three out of the four sites, while the R^2 statistics reveal an acceptable correlation between predicted and observed sediment loads.

More extensive monitoring records were available to assess the predicted $\text{NO}_3\text{-N}$ levels which were close to the observations for several of the gauge sites. The PBIAS values indicated that SWAT either underestimated or overestimated the measured levels. However, the difference was always below 40% with only two exceptions: the Minnesota (Jordan) and Iowa (Wapello) River basins (Table 6). The $\text{NO}_3\text{-N}$ underestimation was quite high during the validation period for these two subregions, and at least for the first one this can be mostly attributed to the underestimation of runoff as discussed previously. However, the PBIAS index was highly acceptable at the most downstream calibration points of both UMRB and OTRB (Grafton and Metropolis respectively), showing that even with some positive or negative deviations at a local basis, the magnitude of total $\text{NO}_3\text{-N}$ loads in the entire region remains acceptable. The NS efficiency is generally lower than for flows; however, the NS statistics calculated for the majority of the gauge sites were positive and over half of the NS and R^2 values exceeded 0.5. The simulated loads were also significantly correlated with observed data as revealed by the R^2 statistics, of which the majority exceeded 0.50, showing that the inter- and intra-annual variability of predictions was reasonable.

The TP statistics were weaker than the $\text{NO}_3\text{-N}$ statistics (Table 6) including an increased number of negative NS values, which reveals a greater uncertainty regarding the TP estimates. However, the PBIAS results were definitely within the acceptable criteria of 40% for all of the gauge sites and simulation periods, except the Jordan validation period, and were very strong at the outlet stations of Grafton and Metropolis. The Grafton and Metropolis NS statistics were relatively weak, but were all positive except for the negative Grafton NS validation value. However, the R^2 statistics were near 0.5 for both outlet stations indicating that SWAT tracked the much of the seasonal trends in the measured data. Overall, the difficulty in obtaining consistently strong monthly statistics for $\text{NO}_3\text{-N}$ and TP is not unexpected given the large scale of application and the uncertainty regarding much of the input data.

Fig. 4 shows graphs of simulated versus observed sediment, $\text{NO}_3\text{-N}$ and TP data for the entire simulation period including both the most recent years used for calibration (1997 and onwards) and those used for validating model performance (before 1996 with length varying based on the availability). The figure includes gauge stations which are indicative of the models' performance. Pollutant loads at the outlets (Grafton and Metropolis) have been well predicted on a monthly basis, while at intermediate outlets there is mostly a mismatch between the highest peaks, which is the main reason for the poorer statistics in these locations discussed above. However, recession limbs and the general shape of the graphs reveal that SWAT predictions do not generally deviate from the observed patterns.

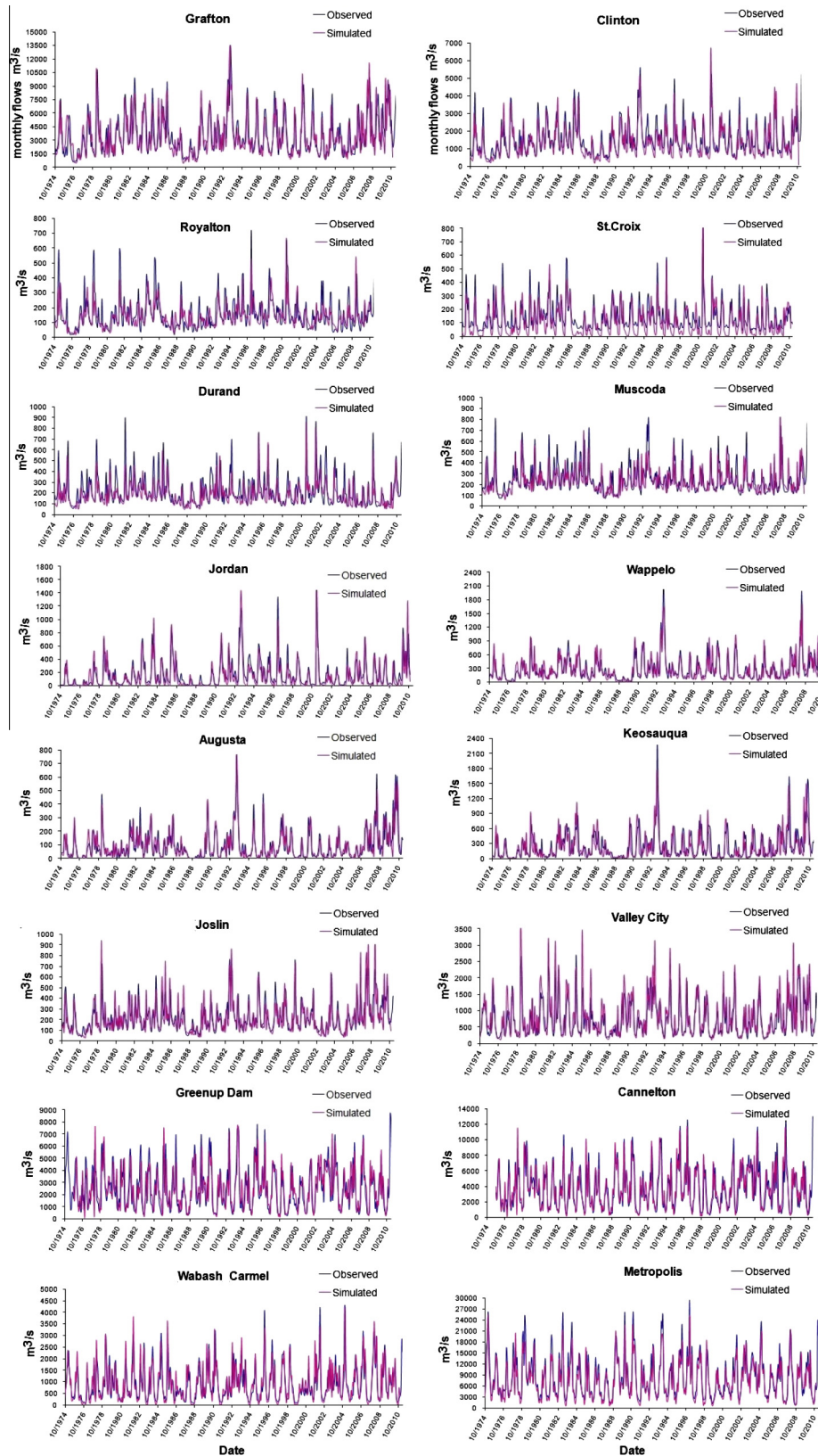


Fig. 3. Monthly simulated versus observed flows at river gauge sites across the Corn Belt. Locations are listed in Table 2 and depicted in Fig. 2.

3.3. A broad-scale overview of the SWAT performance for the Corn Belt region

In this section we further present the SWAT performance on an annual basis for the entire UMRB and OTRB areas in order to

give a clear picture of the results at the large river basin scale. Thus, we refer to the most downstream monitoring sites in the areas (Grafton and Metropolis; see Fig. 2), which are the reference points of the presented annual river-basin scale results.

Table 5

Mean annual (1975–2010) observed, simulated and confidence limits of the observed sediments, TN and TP loads in UMRB and OTRB (all in 1000 tonnes).

| | obs Sed | sim Sed | obs TN | sim TN | obs TN LI | obs TN UI | obs TP | sim TP | obs TP LI | obs TP UI |
|---------------|------------|------------|-----------|-----------|--------------|--------------|-----------|-----------|--------------|--------------|
| Jordan | 1065.0 | 850.0 | 82.3 | 45.6 | 31.1 | 194.1 | 1.3 | 1.8 | 1.0 | 1.7 |
| St. Paul | | | 61.9 | 63.5 | 49.4 | 77.3 | 3.1 | 3.8 | 2.8 | 3.5 |
| Clinton | 4088.0 | 4000.0 | 142.4 | 106.7 | 105.6 | 191.9 | 8.5 | 9.2 | 7.1 | 10.1 |
| Wapello | 2091.9 | 2054.1 | 86.1 | 50.2 | 59.3 | 122.8 | 3.3 | 3.2 | 2.6 | 4.1 |
| Valley City | 4794.4 | 5270.5 | 134.0 | 131.9 | 115.4 | 155.0 | 7.8 | 8.3 | 6.8 | 9.0 |
| Grafton | 21161.0 | 21933.3 | 509.9 | 452.9 | 413.6 | 624.8 | 31.0 | 34.1 | 26.1 | 36.6 |
| Mt. Carmell | 5307.0 | 5520.0 | 132.9 | 135.9 | 103.6 | 168.9 | 7.9 | 7.7 | 6.7 | 9.2 |
| Paducah | | | 40.0 | 28.5 | 31.7 | 50.0 | 4.1 | 4.2 | 3.4 | 4.8 |
| Greenup Dam | | | 122.3 | | | | | | | |
| Cannelton Dam | | | 241.8 | 181.6 | 213.5 | 274.0 | 27.2 | 21.0 | 21.3 | 34.5 |
| Metropolis | 35681.0 | 39400.0 | 498.3 | 428.4 | 415.7 | 594.4 | 47.1 | 48.7 | 38.9 | 56.7 |

obs: observed, sim: simulated, LI: lower interval of the observation, UI: upper interval of the observation.

Table 6

Monthly calibration and validation water quality statistics for the UMRB and OTRB subregions.

| Calibration point (Fig. 2) | Sediments | | | NO ₃ -N | | | | | | TP | | | | | |
|----------------------------|-----------|-------|----------------|--------------------|--------|------|-------|----------------|----------------|--------|--------|-------|-------|----------------|----------------|
| | | | | Cal | | Val | | Cal | | Val | | Cal | | Val | |
| | PBIAS | NS | R ² | PBIAS | PBIAS | NS | NS | R ² | R ² | PBIAS | PBIAS | NS | NS | R ² | R ² |
| Jordan | | | | 6.19 | 56.50 | 0.25 | 0.13 | 0.56 | 0.16 | -6.64 | -45.75 | 0.33 | 0.34 | 0.50 | 0.34 |
| Wapello | 1.81 | 0.54 | 0.61 | 42.08 | 52.03 | 0.38 | 0.16 | 0.54 | 0.39 | -4.99 | 5.38 | -0.19 | 0.32 | 0.56 | 0.62 |
| Augusta | 8.60 | 0.56 | 0.57 | | | | | | | | | | | | |
| Clinton ^a | | | | 20.58 | -9.92 | 0.38 | -0.07 | 0.51 | 0.33 | -27.42 | 13.03 | -1.56 | -0.77 | 0.37 | 0.21 |
| Valley City | -9.93 | -0.53 | 0.56 | 1.12 | -1.64 | 0.60 | 0.56 | 0.61 | 0.60 | 3.55 | -12.05 | -1.92 | -1.04 | 0.32 | 0.44 |
| Grafton ^a | -3.65 | 0.30 | 0.47 | 7.53 | 5.69 | 0.40 | 0.36 | 0.61 | 0.57 | -9.62 | -9.78 | 0.02 | -0.40 | 0.52 | 0.43 |
| Paducah | | | | -8.32 | 22.76 | 0.56 | 0.68 | 0.57 | 0.73 | -12.14 | 4.71 | -0.17 | -0.07 | 0.24 | 0.61 |
| Greenup | | | | 12.28 | 24.07 | 0.61 | 0.46 | 0.73 | 0.74 | 9.70 | 35.38 | 0.54 | 0.29 | 0.53 | 0.45 |
| Mt. Carmel | | | | 0.47 | -28.73 | 0.60 | -0.55 | 0.66 | 0.62 | -5.56 | 15.52 | 0.06 | 0.31 | 0.53 | 0.55 |
| Cannelton ^a | | | | 1.99 | 17.77 | 0.76 | 0.70 | 0.77 | 0.77 | 20.77 | 25.30 | 0.51 | 0.42 | 0.58 | 0.46 |
| Metropolis ^a | | | | -4.90 | 12.49 | 0.72 | 0.61 | 0.75 | 0.63 | -7.64 | -0.51 | 0.37 | 0.36 | 0.49 | 0.44 |

^a These calibration points receive water and pollutants from upstream calibrated watersheds and their water quality calibration was done after calibrating the upstream areas. R² is the coefficient of determination, NS the Nash–Sutcliffe efficiency and PBIAS the percent bias with positive values indicating model underestimations and negative overestimations.

Fig. 5 shows the comparison between the simulated annual flows, NO₃-N and TP loads with the respective observed ones for the entire simulation period (1975–2010). Annual flow predictions for both basins are excellent and are very strongly correlated with the observed flows. On the other hand, annual nutrient loads are well correlated at Grafton (UMRB) but less at Metropolis (OTRB). Table 7 summarizes the annual NS, R² and PBIAS statistics for both of these gauge-sites for the calibration and validation periods.

Absolute PBIAS values are highly acceptable as can be seen in the table as they are consistently lower than 10% for both flows and nutrients in the two regions. The resulting annual flow NS and R² values were above 0.90 for both the calibration and validation periods in the UMRB and for the validation period in the OTRB, showing an excellent match between the SWAT annual predictions and the observations. Moreover, the UMRB NO₃-N NS and R² values were 0.66 and 0.72, respectively, for the calibration period and above 0.80 for the validation period. Here, the aggregation of monthly numbers leads to a significant improvement of SWAT performance at the annual basis, which is the case for almost all monitoring points in the region. The results for TP were quite similar and can be judged as acceptable or marginally acceptable as regards the NS efficiency of the validation period, when the value was below 0.5. For the OTRB, the annual water quality performance of SWAT was somewhat poorer with statistics being however acceptable for the calibration period. The rather low NS and R² statistics of the validation may be associated to a reduced representativeness of the parameterized model for the old years of this period (1975–1996) in the OTRB area.

Table 8 presents the mean annual calibrated water balance components in both basins with reference to the total simulation

period (1975–2010). The mean annual actual ET was 593 and 638 mm for the UMRB and OTRB, representing 68% and the 53% of the annual precipitation, respectively. Total annual runoff in the UMRB (262 mm) is comprised of surface runoff (30%), baseflow (50%) and lateral and tile flow (20%). In the OTRB, the relative contribution is somewhat different, with baseflow representing 40% of the total annual runoff, lateral and tile flow 25%, while surface runoff is almost one third of total runoff. However, tile flow in the OTRB is considerably less as compared to the UMRB, due primarily to the significantly lower amount of agricultural (and tile-drained) land in the basin.

Table 9 demonstrates the annual nutrient source apportionment in both basins as estimated by SWAT. The data included in this table indicate that agricultural diffuse losses are responsible for more than 70% of both the TN and TP losses to surface waters in the UMRB, and approximately 50% in the OTRB. Point sources contributed 16% of the total UMRB N and P loads, in contrast to the corresponding contributions in the OTRB, which exceeded 20% for the total N load but only about 11% for the total P load. Diffuse losses from non-agricultural land (named natural background losses in the table) are quite high in OTRB due to the significantly smaller crop areas compared to the UMRB where cropping systems occupy almost half of the basin's area. The estimates in Table 9 can be considered reliable since point sources are measured numbers (no uncertainty) and diffuse sources of N and P have been resulted from spatially well-parameterized and calibrated models that maintain heterogeneity.

The seasonal hydrologic and nutrient transport regime in the region was also assessed by estimating the mean monthly flows, and TN and TP river loads, for the period 1975–2010 at the most

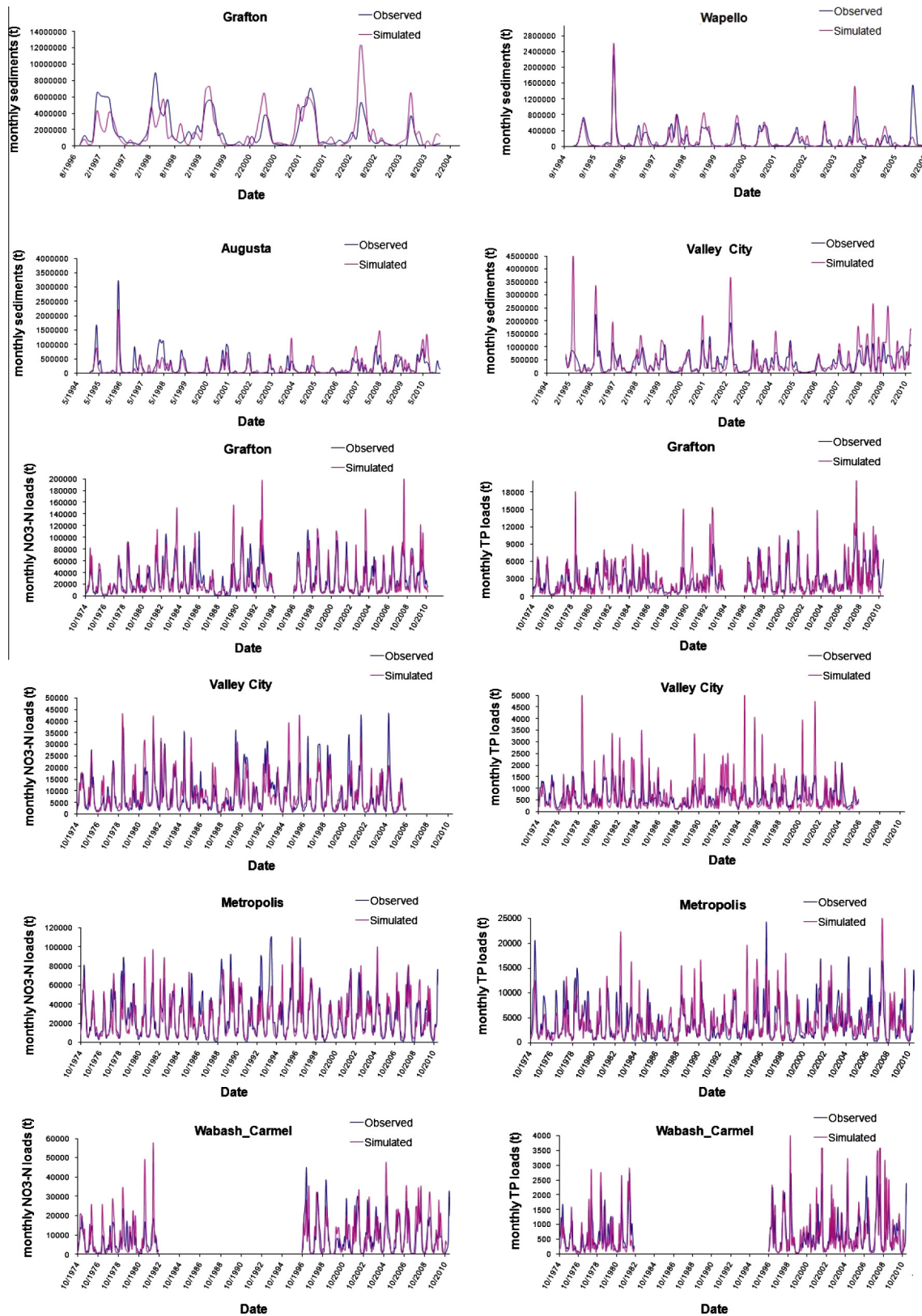


Fig. 4. Monthly simulated versus observed pollutants in several river gauge stations across the Corn Belt. Locations are listed in Table 2 and depicted in Fig. 2.

downstream gauge sites of UMRB and OTRB (Grafton and Metropolis; Fig. 2). Fig. 6 demonstrates this temporal variation. From the graphs it can be clearly concluded that the temporal variation of the TN and TP loads is highly pronounced with the highest simulated loads occurring in late spring/early summer.

This is the most critical period for water pollution due to the combined effect of crop fertilization, highest precipitation amounts, and high tile flow volumes in the basin. With regard to TN, which is mostly comprised of $\text{NO}_3\text{-N}$ associated with sub-surface runoff, April, May and June are also the months with the highest rate of

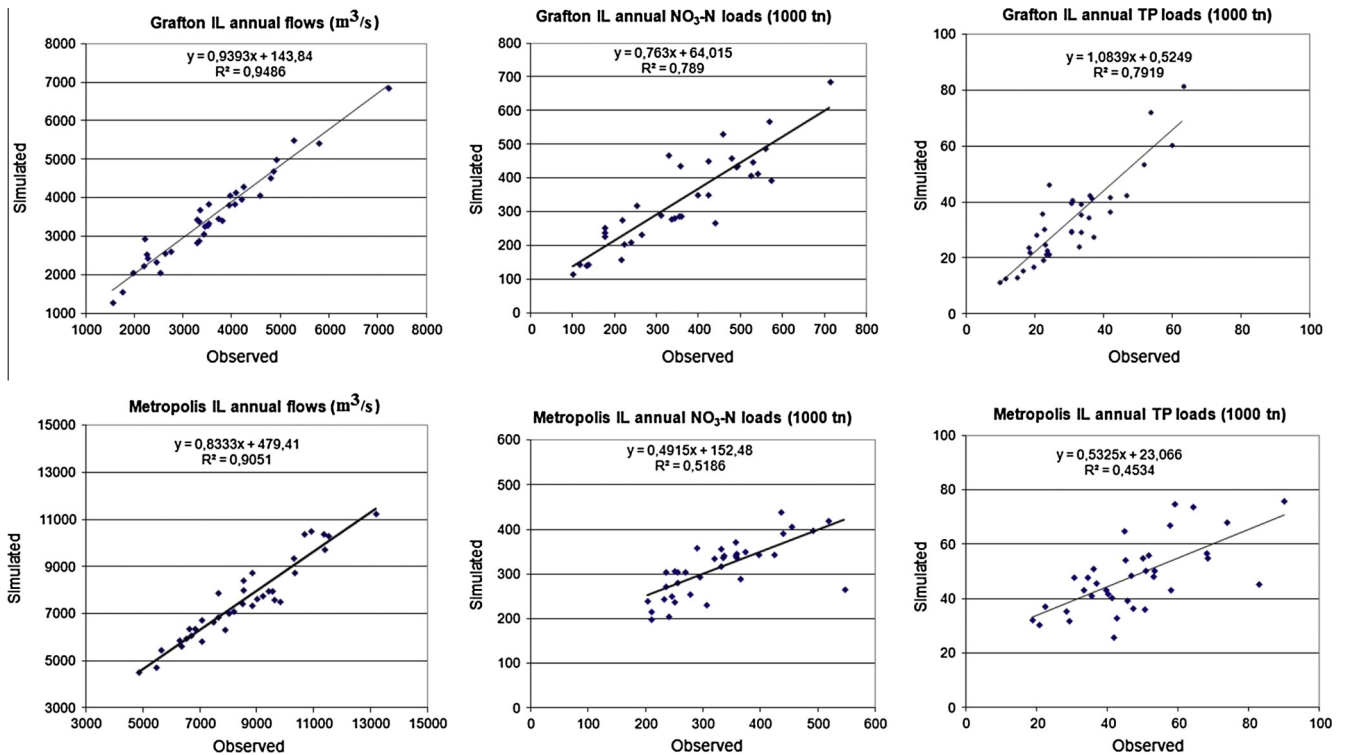


Fig. 5. Annual (1975–2010) comparison of simulated and observed flows, NO₃-N and TP loads at the most downstream monitoring points of the UMRB (Grafton) and OTRB (Metropolis).

Table 7
Annual NS, R² and PBIAS statistics at the UMRB and OTRB outlets.

| | | NS | | R ² | | PBIAS | |
|------|--------------------|-------------------------|------------------------|-------------------------|------------------------|-------------------------|------------------------|
| | | Calibration (1997–2010) | Validation (1975–1996) | Calibration (1997–2010) | Validation (1975–1996) | Calibration (1997–2010) | Validation (1975–1996) |
| UMRB | Flows | 0.95 | 0.94 | 0.95 | 0.95 | 1.91 | 2.08 |
| | NO ₃ -N | 0.66 | 0.81 | 0.72 | 0.80 | 7.71 | 3.97 |
| | TP | 0.78 | 0.41 | 0.89 | 0.67 | -9.74 | -10.46 |
| OTRB | Flows | 0.80 | 0.60 | 0.91 | 0.95 | 6.22 | 13.86 |
| | NO ₃ -N | 0.56 | 0.47 | 0.64 | 0.55 | -4.22 | 8.97 |
| | TP | 0.60 | 0.34 | 0.60 | 0.39 | -7.12 | -0.96 |

Table 8
Water balance components (in mm) on a mean annual basis in UMRB and OTRB.

| | 1975–2010 UMRB | 1975–2010 OTRB |
|--------------------------------|----------------|----------------|
| Precipitation (mm) | 878 | 1194 |
| Snow (mm) | 99 | 81 |
| Surface runoff (mm) | 77 | 159 |
| Lateral flow (mm) | 10 | 97 |
| Tile flow (mm) | 44 | 28 |
| Baseflow (mm) | 131 | 194 |
| Total runoff (mm) | 262 | 478 |
| Actual evapotranspiration (mm) | 593 | 638 |

simulated runoff in the intensely cultivated UMRB. Fig. 6 also includes the observed temporal variation of all variables based on the data obtained (USGS, 2013), showing a general good agreement of the shapes of the graphs in all cases; however, it reveals that N and P observed peaks occur 1–2 months earlier than the simulated ones. This indicates that, as both models predicted well the hydrologic temporal variations, they may require additional calibration with respect to the timing of fertilizer and manure

nutrient inputs in order to better capture the temporal variability of nutrient loads. Such information may also increase all monthly nutrient statistics presented previously but needs extensive collaboration with stakeholders to be reliably defined in such a large region.

3.4. Mapping results across the Corn Belt

The water yield and pollution pattern across the UMRB and OTRB is finally presented in Fig. 7 demonstrating the spatial differentiation of water, sediment and nutrient losses at the HRU (12-digit) scale. The simulated annual runoff was very high in parts of the OTRB, especially the northwestern and central part. The generated runoff in the UMRB was significantly lower on a mean annual basis and is minimized in the north and north-western part, especially in the area of the Minnesota River basin where annual precipitation depths are also the minimum within the entire Corn Belt region (~700 mm). On the other hand, sediments originate from many areas across the landscape but most importantly from the agricultural land of Iowa, Illinois, Indiana and Ohio. The majority of erosion factors excluding management (climate, surface runoff, slopes) are considered to have been quite accurately

Table 9
Source apportionment of TN and TP loads in UMRB and OTRB (1975–2010).

| | UMRB ^a | | | | OTRB ^a | | | |
|--|-------------------|------|---------|------|-------------------|------|---------|------|
| | TN (kg) | % TL | TP (kg) | % TL | TN (kg) | % TL | TP (kg) | % TL |
| Point sources | 73,761 | 16.3 | 5404 | 15.9 | 87,237 | 20.4 | 5562 | 11.4 |
| Agricultural diffuse losses | 329,039 | 72.6 | 24,612 | 72.2 | 213,343 | 49.8 | 21,021 | 43.2 |
| Natural background diffuse losses (forest, hay, pasture, etc.) | 50,124 | 11.1 | 4050 | 11.9 | 127,542 | 29.8 | 22,065 | 45.4 |
| Total Losses (TL) | 452,924 | 100 | 34,066 | 100 | 428,122 | 100 | 48,648 | 100 |

^a Based on simulated loads at Grafton for the UMRB and Metropolis for the OTRB (Fig. 2).

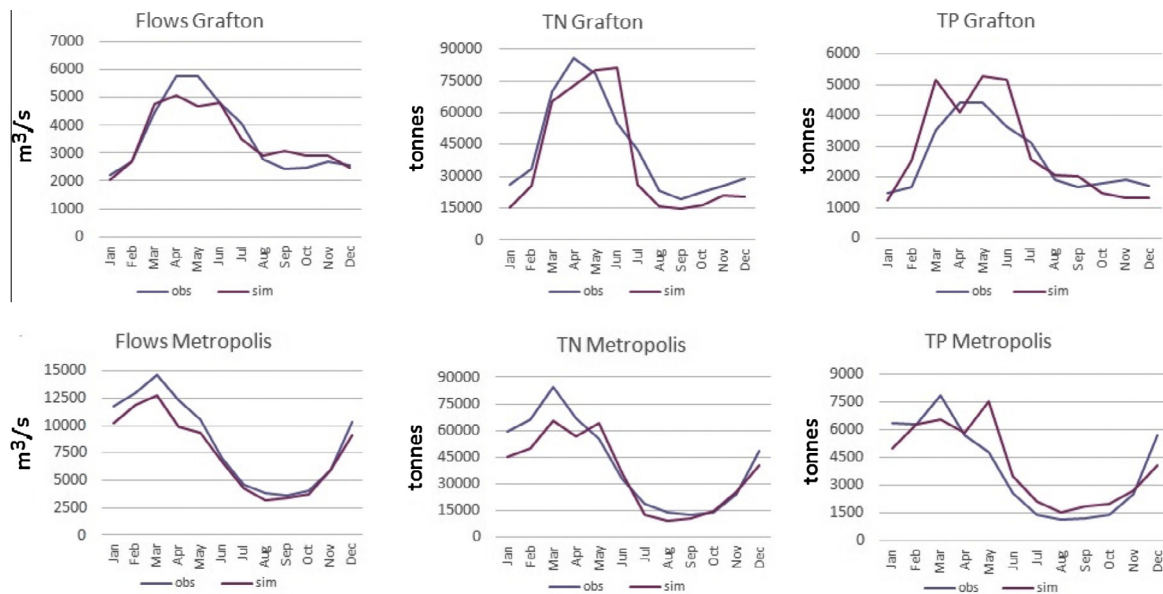


Fig. 6. Temporal variation of observed and simulated flow, TN and TP at the most downstream monitoring points of UMRB (Grafton) and OTRB (Metropolis).

assigned across the landscape to support the validity of this map, which indicates the 12-digit areas with the highest susceptibility to erosion. However, some management information such as the distribution of different tillage practices (conservation, non-conservation), which is one of the factors governing erosion, were applied randomly within each 8-digit watershed.

Fig. 7 includes the TN and TP loads occurring annually in the region. Apart from runoff and erosion mechanisms, N and P pressures play a significant role in the definition of the most vulnerable areas in nutrient losses to waters. SWAT calculated significantly higher TN and TP losses from the agricultural HRUs, where nutrients are applied to row crops. Geomorphological and hydrometeorological factors subsequently govern the magnitude of pollutant losses from these areas, which are mainly concentrated in the same areas with erosion vulnerability for TP as well as in the Des Moines lobe in Iowa and the upstream part of the Wabash River in Indiana and Ohio for TN. The TP map indicates the strong linkage of sediment and P losses in SWAT, while the TN map reveals the role of tile drainage in N losses, which rapidly transfers leached $\text{NO}_3\text{-N}$ to streams and rivers. The areas with high tile drainage density are mostly concentrated in central and northern Iowa, Indiana, western Ohio and central Illinois, where the greatest N losses were simulated.

If these maps are studied in detail, HRUs (12-digit watersheds) with substantially different sensitivity in losses of various kinds of pollutants can be identified. Thus, an HRU with very high vulnerability in P losses may be of moderate vulnerability in N losses. This can be attributed less to the uneven N and P input to this HRU and more to the different mechanisms governing N and P movement on the land, which are associated with surface and subsurface

pathways of pollutant transport. Such differences are crucial for the selection of appropriate management alternatives, which should be selected according to the environmental target (kind of pollutant) that policy makers set as an objective.

Further, Fig. 7 provides the mean annual corn and soybean yields predicted by SWAT in the Corn Belt Region. Corn yield is clearly greater within the State of Iowa, especially in the Des Moines lobe as well as in scattered areas across Minnesota and the States lying within the OTRB. In all these areas corn production exceeds 10 t/ha/y. Soybean yield on the other hand exceeds the value of 3 t/ha/y. In this particular case however, the model maintained the highest yields across a wider area within the Corn Belt including significant areas of all States in the region. This can be attributed to the fact that as a legume, soybean does not meet N stress in areas with significant runoff and N leaching such as those in the eastern Corn Belt, namely the areas within the OTRB.

3.5. Discussion and recommendations on large scale integrated modeling

To the best of our knowledge the present study is the first to report an extensive evaluation of SWAT hydrologic results on a monthly basis and at multiple sites within the wider UMRB and OTRB areas, compared to previous studies that reported hydrologic performance numbers either at a coarser time step and/or at a limited number of gauge sites (Demissie et al., 2012; Jha et al., 2006, 2013; Kannan et al., 2008; Srinivasan et al., 2010; Santhi et al., 2008, 2014; Secchi et al., 2011; Wang et al., 2011; Wu et al., 2012a, 2012b). This study is also the first which is based on a 12-digit model development to such a large spatial extent and

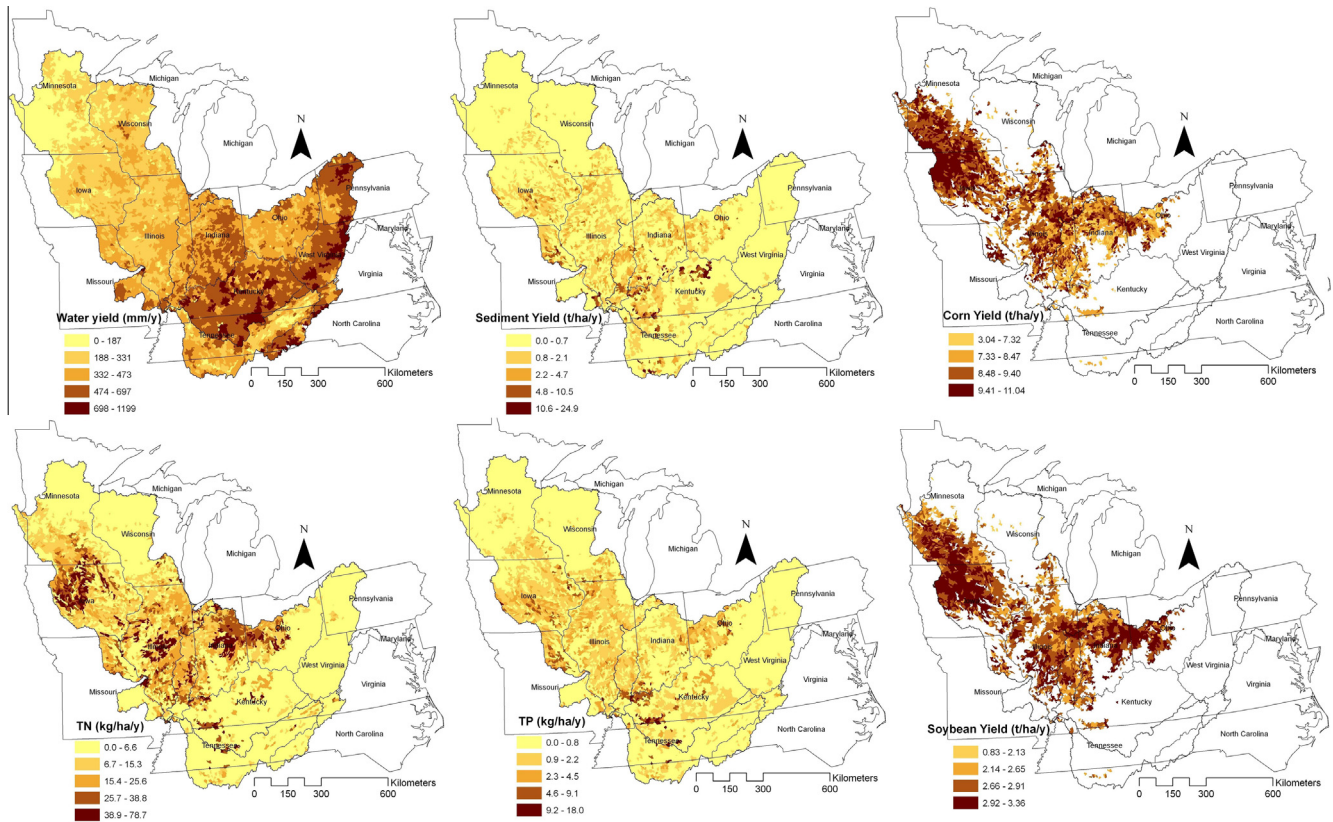


Fig. 7. Mean annual water yield, sediments, TN and TP loads to the surface water system of UMRB and OTRB as well as average corn and soybean yields per 12-digit subbasin as simulated by SWAT within the entire simulation period 1975–2010.

presents the most extensive assessment of aggregated SWAT monthly pollutant estimates performed to date for these two regions. For example, [Santhi et al. \(2014\)](#) reported only mean annual estimates of sediments and nutrients for the OTRB with similar SWAT performance to our models. On the other hand, [Secchi et al. \(2011\)](#) presented annual R^2 and NS statistics only for Grafton in the UMRB with marginally acceptable values for an annual time step. [Zhang and Wu \(2013\)](#) also reported SWAT results only at Grafton, which is the only previous study presenting water quality results on a monthly basis. However, the graphs they present for suspended sediments, TN and TP show a clear mismatch between observed and simulated peaks. [Jha et al. \(2013\)](#) on the other hand, reported mean annual N loadings from the 8-digit HUCs of the UMRB and compared them with the respective SPATIALLY Referenced Regressions On Watershed attributes (SPARROW) predictions, showing a relatively weak correlation, in part due to the lack of accounting for manure applications.

Within the extensive presentation of this modeling effort we tried to share our experiences with data manipulation, model development and results evaluation. A clear objective of this paper however, is to end with a list of recommendations for large scale SWAT modeling either in the Corn Belt or everywhere around the globe. This list is presented next in the form of critical discussion points related to the modeling presented.

- The use of 12-digit watersheds to model the large Corn Belt region in the US assisted the model to capture the key information of climate and topography and provide acceptable hydrologic and water quality estimates all across the region. Given the increased accuracy in capturing climate and slope differentiation it seems that the '12-digit and dominant HRU' option used in this study is better even if land complexity is similar or a bit coarser compared to the option of having bigger subbasins

with multiple HRUs. Moreover, given the resolution of the available soil and management data in the region (and mostly in every large scale project) we do not see the need for the division of the 12-digit watersheds into multiple HRUs at this stage. Soils are coarse and most management data types (fertilizers, tillage, conservation practices, tiles) are not available at a more refined spatial scale other than the 8-digit watershed level. Therefore, to introduce HRUs within the current 12-digit watershed of the project we would need the more detailed SSURGO soils for the US as well as more detailed and reliable management information such as fertilization rates, tile drainage, tillage types and other conservation practices, from extensive surveys across the area.

- In our opinion the use of 8-digits for modeling these large areas does not make sense any more given the large number of precipitation stations located in the area, the resolution of the available digital elevation models and the progress that has been done with SWAT versions and interfaces in supporting large watershed projects. Subbasins in SWAT govern mostly hydrologic processes with climate, slopes and routing processes being associated with their number/size/location, thus, it is advisable, when possible, to rely on a large number of subbasins in SWAT projects instead of large number of HRUs.
- Calibration of such large and detailed watershed schematized projects need however efficient approaches and tools. The Sequential Uncertainty Fitting algorithm embedded in the auto-calibration and uncertainty analysis SWAT-CUP program can facilitate the calibration of such models in reasonable time and at multiple locations simultaneously, which is generally unfeasible by following a manual approach. As proved from the results of this study, SWAT-CUP is an indispensable tool for identifying the magnitude of hydrologic processes across different parts of large river basins by narrowing the uncertainty of predictions.

- On the other hand, SWAT water quality calibration is recommended to be done manually (no-automatically). One reason is that water quality (sediments, nutrients) is governed by parameters that are defined at the entire basin level, thus, an automatic calibration at several gauge-sites is not very useful. A manual calibration keeps the model manipulation under control preventing the user from being lost in highly uncertain paths. From our analysis it is also shown that although SWAT contains a large amount of water quality parameters, in practice only a few of them are sensitive and very useful in calibration. This may be attributed to the reduced ability of the model to simulate pollutant transport compared to hydrology and its shortcomings in appropriately considering the effect of specific parameters on water quality simulations, such as for example, the initial levels of nutrient pools in soils.
- To evaluate water quality performance of SWAT at a very large scale we also recommend the use of the PBIAS index as a first evaluation criterion. In such large projects what is of utmost importance is to ensure that predictions are within a good range of observations instead of simulating a very successful graph. Pollutant load dynamics, although important, are more difficult to predict and what can be more reliably addressed is the accumulated load within a specific time period. This is however appropriate to address several environmental problems such as the water quality degradation of water bodies and estuaries, for example the gulf of Mexico hypoxia (Kling et al., 2014).
- To this end, the consideration of maps showing spatial differentiation of a variable across large areas can be more reliable (reduced uncertainty) when these maps depict annual or mean annual estimates. Even if the depicted data (absolute values) of these maps include uncertainty they are highly informative in showing the relative importance of an area in water pollution or crop growth compared to others. This study strongly agrees with the consideration of SWAT as a powerful tool for spatially allocating pollutant loads and crop yields under large time steps when appropriately parameterized (Niraula et al., 2012; Panagopoulos et al., 2011), while this argument becomes stronger with the 12-digit schematization of the Corn Belt area due to the detailed consideration of climate and slope variability. In the particular case of the depicted crop yields, uncertainties may increase due to other factors such as the inability of the model to consider pest diseases in specific areas and years or genetic improvements of crop varieties that have resulted in increased yields in areas of low productivity.
- This study also tried to face reservoir operation difficulties. We found that reservoir water quality simulation in SWAT with the use of the settling rate parameters has severe problems of rationality. However, the fact that most reservoirs in the study region have not water supply as primary purpose (they have the production of hydroelectricity, navigation or flood control) implies that no water is practically lost from its natural path. This can support the decision in this study to exclude pollutant trapping simulation in the reservoirs by deactivating them. As water from the reservoirs in the Corn Belt is released downstream rather frequently, it can be assumed that both sediments and nutrients have no significant time to be settled and are mostly transported downstream. However, reservoirs operation should definitely be improved in SWAT to be able to simulate properly their potential impact on pollutant transport. To this end, real and frequent measurements upstream and downstream reservoirs should be conducted to relate inflows, reservoir characteristics and operation rules with measured outflows. Given our gained experience the simulation of reservoirs is not suggested in water quality SWAT studies.
- Finally, it would also be ideal to have complete time-series of measured pollutant loads all across the Corn Belt region. Due

to the reduced length of observed data in some stations the uncertainty of model predictions increases there. However, for such a large area and long simulation period we are rather satisfied with the data obtained, while the use of PBIAS to evaluate our estimations can face the problem of data length in some circumstances. The use of other evaluation indices is certainly recommended in future updates of the current model.

4. Summary and conclusions

This study presented a refined SWAT modeling approach for the Corn Belt region of the Midwestern US, which was based on an efficient combination of a semi-automatic hydrologic calibration and uncertainty analysis and a manual water quality calibration, appropriate for large-scale projects. One key point of the present research is that the calibration and validation of such large hydrologic systems is an intensive task, which can be gradually improved as more accurate data and improved model algorithms become available, allowing more robust assumptions of reality. Incorporation of HRUs within the 12-digit subwatersheds is an important future improvement which will allow better representation of different combinations of cropland landscapes, soils and management practices within the two simulated regions when detailed layers of these data are disclosed. It is anticipated that the needed improvements in several SWAT routines in combination with the improved representation of existing conservation practices, wetlands, and reservoirs, fertilizer and manure inputs, and other refined inputs such as the use of SSURGO soil data, will improve the current large modeling effort and should be incorporated in the future versions of the models.

In the UMRB and OTRB, both flow and pollutant predictions at the monthly basis were in most cases impressively good given the size and the complexity of the landscape simulated. Thus, the first complete phase of calibration and validation results presented in this study underscore that the system can replicate the key hydrologic and nutrient loss dynamics occurring in the basins. The 12-digit watershed based modeling system that has been developed promises to enhance targeting of cropping systems and management practices on sensitive cropped landscapes in relation to local water quality issues and the seasonal hypoxic zone that forms annually in the northern Gulf of Mexico. It is believed that despite possible limitations and needs for improvements, the current modeling system provides a reliable approach to support the evaluation of environmental and economic impacts of agricultural management in the Corn Belt under existing and future climates, and the identification of possible implications for all interested parties.

Acknowledgments

This research was partially funded by the National Science Foundation, Award No. DEB1010259, Understanding Land Use Decisions & Watershed Scale Interactions: Water Quality in the Mississippi River Basin & Hypoxic Conditions in the Gulf of Mexico, by the US Department of Agriculture, National Institute of Food and Agriculture, Award No. 20116800230190, Climate Change, Mitigation, and Adaptation In Corn-Based Cropping Systems, and by the US Environmental Protection Agency's Science to Achieve Results (STAR) award (EPA G 1469 1 2008 35615 04666). USDA is an equal opportunity provider and employer.

References

- Abbaspour, K.C., 2012. User Manual for SWAT-CUP 5.1.4. SWAT Calibration and Uncertainty Analysis Programs – A User Manual. Swiss Federal Institute of

- Aquatic Science and Technology, Eawag, Duebendorf, Switzerland, 103pp. <<http://www.neprashtechology.ca/Downloads.aspx>>.
- Abbaspour, K.C., Yang, J., Maximov, I., Siber, R., Bogner, K., Mieleitner, J., Zobrist, J., Srinivasan, R., 2007. Modelling hydrology and water quality in the pre-alpine/alpine Thur watershed using SWAT. *J. Hydrol.* 333, 413–430.
- Arabi, M., Frankenberger, J.R., Engel, B.A., Arnold, J.G., 2008. Representation of agricultural conservation practices with SWAT. *Hydrol. Process.* 22 (16), 3042–3055. <http://dx.doi.org/10.1002/hyp.6890>.
- Arnold, J.G., Srinivasan, R., Muttiah, R.S., Williams, J.R., 1998. Large area hydrologic modeling and assessment Part I: Model development. *J. Am. Water Resour. Assoc.* 34 (1), 73–89. <http://dx.doi.org/10.1111/j.1752-1688.1998.tb05961.x>.
- Arnold, J.G., Allen, P.M., Volk, M., Williams, J.R., Bosch, D.D., 2010. Assessment of different representations of spatial variability on SWAT model performance. *Trans. ASABE* 53 (5), 1433–1443.
- Arnold, J.G., Moriasi, D.N., Gassman, P.W., Abbaspour, K.C., White, M.J., Srinivasan, R., Santhi, C., Harmel, R.D., van Griensven, A., Van Liew, M.W., Kannan, N., Jha, M.K., 2012. SWAT: model use, calibration, and validation. *Trans. ASABE* 55 (4), 1491–1508.
- Baker, N.T., 2011. Tillage Practices in the Conterminous United States, 1989–2004—Datasets Aggregated by Watershed. Data Series 573. U.S. Geological Survey, Reston, Virginia. <<http://pubs.usgs.gov/ds/ds573/>>.
- Belmont, P., Gran, K.B., Schottler, S.P., Wilcock, P.R., Day, S.S., Jennings, C., Lauer, J.W., Viparelli, E., Willenbring, J.K., Engstrom, D.R., Parker, G., 2011. Large shift in source of fine sediment in the upper Mississippi River. *Environ. Sci. Technol.* 45, 8804–8810. <http://dx.doi.org/10.1021/es2019109>.
- Bosch, D.D., Arnold, J.G., Volk, M., Allen, P.M., 2010. Simulation of a low-gradient coastal plain watershed using the SWAT landscape model. *Trans. ASABE* 53 (5), 1445–1456.
- David, M.B., Del Grosso, S.J., Hu, X., Marshall, E.P., McIsaac, G.F., Parton, W.J., Tonitto, C., Youssef, M.A., 2009. Modeling denitrification in a tile-drained, corn and soybean agroecosystem of Illinois, USA. *Biogeochemistry* 93, 7–30. <http://dx.doi.org/10.1007/s10533-008-9273-9>.
- David, M.B., Drinkwater, L.E., McIsaac, G.F., 2010. Sources of nitrate yields in the Mississippi River Basin. *J. Environ. Qual.* 39, 1657–1667. <http://dx.doi.org/10.2134/jeq2010.0115>.
- Demissie, Y., Yan, E., Wu, M., 2012. Assessing regional hydrology and water quality implications of large-scale biofuel feedstock production in the upper Mississippi river basin. *Environ. Sci. Technol.* 46, 9174–9182. <http://dx.doi.org/10.1021/es300769k>.
- Douglas-Mankin, K.R., Srinivasan, R., Arnold, J.G., 2010. Soil and Water Assessment Tool (SWAT) model: current developments and applications. *Trans. ASABE* 53 (5), 1423–1431.
- Duriancik, L.F., Bucks, D., Dobrowolski, J.P., Drewes, T., Eckles, S.D., Jolley, L., Kellogg, R.L., Lund, D., Makuch, J.R., O'Neill, M.P., Rewa, C.A., Walbridge, M.R., Parry, R., Weltz, M.A., 2008. The first five years of the Conservation Effects Assessment Project. *J. Soil Water Conserv.* 63 (6), 185A–197A. <http://dx.doi.org/10.2489/jswc.63.6.185A>.
- EPA-SAB (Environmental Protection Agency – Science Advisory Board), 2007. <http://www.epa.gov/msbasin/pdf/sab_report_2007.pdf>.
- Gassman, P.W., Reyes, M.R., Green, C.H., Arnold, J.G., 2007. The Soil and Water Assessment Tool: historical development, applications, and future research directions. *Trans. ASABE* 50 (4), 1211–1250.
- Gassman, P.W., Sadeghi, A.M., Srinivasan, R., 2014. Applications of the SWAT Model Special Section: overview and insights. *J. Environ. Qual.* 43 (1), 1–8. <http://dx.doi.org/10.2134/jeq2013.11.0466>.
- IPNI, 2010. A Preliminary Nutrient Use Geographic Information System (NuGIS) for the U.S. International Plant Nutrition Institute (IPNI), Norcross, GA. <<http://www.ipni.net/nugis>>.
- Jha, M., Arnold, J.G., Gassman, P.W., Giorgi, F., Gu, R.R., 2006. Climate change sensitivity assessment on Upper Mississippi River Basin streamflows using SWAT. *J. Am. Water Resour. Assoc.* 42 (4), 997–1016. <http://dx.doi.org/10.1111/j.1752-1688.2006.tb04510.x>.
- Jha, M.K., Gassman, P.W., Panagopoulos, Y., 2013. Regional changes in nitrate loadings in the Upper Mississippi River Basin under predicted mid-century climate. *Reg. Environ. Change.* <http://dx.doi.org/10.1007/s10113-013-0539-y>.
- Kannan, N., Santhi, C., Arnold, J.G., 2008. Development of an automated procedure for estimation of the spatial variation of runoff in large river basins. *J. Hydrol.* 359, 1–15.
- Kling, C.L., Panagopoulos, Y., Rabotyagov, S., Valcu, A., Gassman, P.W., Campbell, T., White, M., Arnold, J.G., Srinivasan, R., Jha, M.K., Richardson, J., Moskal, L.M., Turner, G., Rabalais, N., 2014. LUMINATE: linking agricultural land use, local water quality and Gulf of Mexico Hypoxia. *Eur. Rev. Agric. Econ.* 1–29. <http://dx.doi.org/10.1093/erae/jbu009>.
- Krause, P., Boyle, D.P., Båse, F., 2005. Comparison of different efficiency criteria for hydrological model assessment. *Adv. Geosci.* 5, 89–97. <http://dx.doi.org/10.5194/adgeo-5-89-2005>.
- Lenhart, T., Eckhardt, K., Fohrer, N., Frede, H.-G., 2002. Comparison of two different approaches of sensitivity analysis. *Phys. Chem. Earth* 27 (9–10), 645–654.
- Maupin, M.A., Ivahnenko, T., 2011. Nutrient loadings to streams of the continental United States from municipal and industrial effluent. *J. Am. Water Resour. Assoc.* 47 (5), 950–964. <http://dx.doi.org/10.1111/j.1752-1688.2011.00576.x>.
- Mississippi River/Gulf of Mexico Watershed Nutrient Task Force, 2008. Gulf Hypoxia Action Plan 2008 for Reducing, Mitigating, and Controlling Hypoxia in the Northern Gulf of Mexico and Improving Water Quality in the Mississippi River Basin, Washington DC.
- Moriasi, D.N., Arnold, J.G., Liew, M.W., Bingner, R.L., Harmel, R.D., Veith, T.L., 2007. Model evaluation guidelines for systematic quantification of accuracy in watershed simulations. *Trans. ASABE* 50 (3), 885–900.
- Moriasi, D.N., Wilson, B.N., Douglas-Mankin, K.R., Arnold, J.R., Gowda, P.H., 2012. Hydrologic and water quality models: use, calibration and validation. *Trans. ASABE* 55 (4), 1241–1247.
- NCDC-NOAA, 2013. National Climatic Data Center Website: <<http://www.ncdc.noaa.gov/>>.
- Neitsch, S.L., Arnold, J.G., Kiniry, J.R., Williams, J.R., 2009. Soil and Water Assessment Tool (SWAT) Theoretical Documentation. Blackland Research Center, Texas. Agricultural Experiment Station, Temple, Texas (BRC Report 02-05). <<http://swatmodel.tamu.edu/documentation>>.
- Niraula, R., Kalin, L., Wang, R., Srivastava, P., 2012. Determining nutrient and sediment critical source areas with SWAT: effect of lumped calibration. *Trans. ASABE* 55 (1), 137–147.
- NLCD, 2001. <<http://www.asprs.org/publications/pers/2007journal/april/highlight.pdf>>.
- Pagliero, L., Bouraoui, F., Willems, P., Diels, J., 2014. Large scale hydrological simulations using SWAT, protocol development and application in the Danube Basin. *J. Environ. Qual.* 43 (1), 145–154. <http://dx.doi.org/10.2134/jeq2011.0359>.
- Panagopoulos, Y., Makropoulos, C., Baltas, E., Mimikou, M., 2011. SWAT parameterization for the identification of critical diffuse pollution source areas under data limitations. *Ecol. Model.* 222 (19), 3500–3512.
- Panagopoulos, Y., Gassman, P.W., Arriitt, R., Herzmann, D.E., Campbell, T., Jha, M.K., Kling, C., Srinivasan, R., White, M., Arnold, J.G., 2014. Surface water quality and cropping systems sustainability under a changing climate in the upper Mississippi river basin. *J. Soil Water Conserv.* 69 (6), 483–494. <http://dx.doi.org/10.2489/jswc.69.6.483>.
- Rabalais, N.N., Turner, R.E., Gupta, B.K.S., Boesch, D.F., Chapman, P., Murrell, M.C., 2007. Hypoxia in the northern Gulf of Mexico: does the science support the plan to reduce, mitigate, and control hypoxia? *Estuar. Coasts* 30 (5), 753–772.
- Rabotyagov, S., Campbell, T., Jha, M.K., Gassman, P.W., Arnold, J.G., Kurkalova, L., Secchi, S., Feng, H., Kling, C.L., 2010. Least cost control of agricultural nutrient contributions to the Gulf of Mexico Hypoxic Zone. *Ecol. Appl.* 20 (6), 1542–1555. <http://dx.doi.org/10.1890/08-0680>.
- Rathjens, H., Oppelt, N., Bosch, D.D., Arnold, J.G., Volk, M., 2014. Development of a grid-based version of the SWAT landscape model. *Hydrol. Process.* <http://dx.doi.org/10.1002/hyp.10197>.
- Rossi, C.G., Srinivasan, R., Jirayot, K., Le Due, T., Souvannabouth, P., Binh, N., Gassman, P.W., 2009. Hydrologic evaluation of the lower Mekong River basin with the Soil and Water Assessment Tool model. *Int. Agric. Eng. J.* 18 (1–2), 1–13.
- Runkel, R.L., Crawford, C.G., Cohn, T.A., 2004. Load Estimator (LOADEST): A FORTRAN Program for Estimating Constituent Loads in Streams and Rivers: U.S. Geological Survey Techniques and Methods Book 4, Chapter A5. U.S. Department of the Interior, U.S. Geological Survey, Reston, VA. <<http://water.usgs.gov/software/loadest/doc/>>.
- Santhi, C., Kannan, N., Arnold, J.G., Di Luzio, M., 2008. Spatial calibration and temporal validation of flow for regional scale hydrologic modeling. *J. Am. Water Resour. Assoc.* 44 (4), 829–846.
- Santhi, C., Kannan, N., White, M., Di Luzio, M., Arnold, J.G., Wang, X., Williams, J.R., 2014. An integrated modeling approach for estimating the water quality benefits of conservation practices at the river basin scale. *J. Environ. Qual.* 43 (1), 177–198. <http://dx.doi.org/10.2134/jeq2011.0460>.
- Sawyer, J., 2012. Nitrogen use in corn production. In: 2012 Crop Advantage Series. Iowa State Univ. Ext., Ames, p. 12. <<http://www.agronext.iastate.edu/soilfertility/info/07CAScornsheet.pdf>>.
- Schilling, K.E., Wolter, C.F., 2009. Modeling nitrate–nitrogen load reduction strategies for the Des Moines River, Iowa using SWAT. *Environ. Manage.* 44 (4), 671–682. <http://dx.doi.org/10.1007/s00267-009-9364-y>.
- Schilling, K.E., Isenhardt, T.M., Palmer, J.A., Wolter, C.F., Spooner, J., 2011. Impacts of land-cover change on suspended sediment transport in two agricultural watersheds. *JAWRA J. Am. Water Resour. Assoc.* 47, 672–686. <http://dx.doi.org/10.1111/j.1752-1688.2011.00533.x>.
- Schuol, J., Abbaspour, K.C., Srinivasan, R., Yang, H., 2008a. Estimation of freshwater availability in the West African sub-continent using the SWAT hydrologic model. *J. Hydrol.* 352 (1–2), 30–49. <http://dx.doi.org/10.1016/j.jhydrol.2007.12.025>.
- Schuol, J., Abbaspour, K.C., Yang, H., Srinivasan, R., Zehnder, A.J.B., 2008b. Modeling blue and green water availability in Africa. *Water Resour. Res.* 44 (W07406), 1–18. <http://dx.doi.org/10.1029/2007WR006609>.
- Secchi, S., Gassman, P.W., Jha, M.K., Kurkalova, L., Kling, C.L., 2011. Potential water quality changes due to corn expansion in the Upper Mississippi River Basin. *Ecol. Appl.* 21 (4), 1068–1084. <http://dx.doi.org/10.1890/09-0619.1>.
- Srinivasan, R., Zhang, X., Arnold, J., 2010. SWAT ungauged: hydrological budget and crop yield predictions in the Upper Mississippi River Basin. *Trans. ASABE* 53 (5), 1533–1546.
- Sugg, Z., 2007. Assessing U.S. Farm Drainage: Can GIS Lead to Better Estimates of Subsurface Drainage Extent? World Resources Institute, Washington, DC. <<http://www.wri.org/publication/assessing-us-farm-drainage-can-gis-lead-better-estimates-subsurface-drainage-exten>>.
- SWAT, 2013. ArcSWAT: ArcGIS-ArcView Extension and Graphical User Input Interface for SWAT. U.S. Department of Agriculture, Agricultural Research Service, Grassland, Soil & Water Research Laboratory, Temple, TX. <<http://swat.tamu.edu/software/arcs SWAT/>>.

- Tuppad, P., Douglas-Mankin, K.R., Lee, T., Srinivasan, R., Arnold, J.G., 2011. Soil and Water Assessment Tool (SWAT) hydrologic/water quality model: extended capability and wider adoption. *Trans. ASABE* 54 (5), 1677–1684.
- Turner, R.E., Rabalais, N.N., Justic, D., 2008. Gulf of Mexico hypoxia: alternate states and a legacy. *Environ. Sci. Technol.* 42 (7), 2323–2327.
- USACE, 2012. CorpsMap: National Inventory of Dams. Washington, DC: US Army Corps of Engineers. <<http://geo.usace.army.mil/pgis/f?p=397:1:0>>.
- USDA Biofuels Strategic Production Report, 2010. A USDA Regional Roadmap to Meeting the Biofuels Goals of the Renewable Fuels Standard by 2022. <http://www.usda.gov/documents/USDA_Biofuels_Report_6232010.pdf> (accessed 10.11.10).
- USDA-NASS, 2013. CDL Online Website: <<http://www.nass.usda.gov/research/Cropland/SARS1a.htm>>.
- USDA-NRCS, 2011. Assessment of the Effects of Conservation Practices on Cultivated Cropland in the Ohio-Tennessee River Basin (November 2011). The Conservation Effects Assessment Project, Official Report, p. 175. <http://www.nrcs.usda.gov/Internet/FSE_DOCUMENTS/stelprdb1046342.pdf>.
- USDA-NRCS, 2012. Assessment of the Effects of Conservation Practices on Cultivated Cropland in the Upper Mississippi River Basin (Revised JULY 2012). The Conservation Effects Assessment Project, Official Report, p. 189. <http://www.nrcs.usda.gov/Internet/FSE_DOCUMENTS/stelprdb1042093.pdf>.
- USDA-NRCS, 2013. Soil Web Portal. <<http://soildatamart.nrcs.usda.gov/>>.
- USEPA (U.S. Environmental Protection Agency), 1998. National Strategy for the Development of Regional Nutrient Criteria: Office of Water, EPA-822-R-98-002, 47pp.
- USEPA (U.S. Environmental Protection Agency), 2000. Nutrient Criteria Technical Guidance Manual-Lakes and Reservoirs: Office of Water, EPA-822-B-00-001, 238pp.
- USEPA SAB [U.S. Environmental Protection Agency, Science Advisory Board], 2007. Hypoxia in the Northern Gulf of Mexico: An Update by the EPA Science Advisory Board. EPA-SAB-08-004. EPA Science Advisory Board, U.S. Environmental Protection Agency, Washington, DC, USA.
- USGS, 2012. Federal Standards and Procedures for the National Watershed Boundary Dataset (WBD). Techniques and Methods 11-A3, Chapter 3 of Section A, Federal Standards Book 11, Collection and Delineation of Spatial Data, third ed. U.S. Department of the Interior, U.S. Geological Survey, Reston, VA and U.S. Department of Agriculture, Natural Resources Conservation Service, Washington, DC. <<http://pubs.usgs.gov/tm/tm11a3/>>.
- USGS, 2013. Online Water Quantity and Quality Data Website: <<http://waterwatch.usgs.gov/wqwatch/>> and Online National Elevation Data Website: <<http://ned.usgs.gov/>>.
- USGS, 2014a. Hydrologic Unit Maps. U.S. Department of the Interior, U.S. Geological Survey, Reston, VA. <<http://water.usgs.gov/GIS/huc.html>>.
- USGS, 2014b. Load Estimator (LOADEST): A Program for Estimating Constituent Loads in Streams and Rivers. U.S. Department of the Interior, U.S. Geological Survey, Reston, VA. <<http://water.usgs.gov/software/loadest/>>.
- Van Griensven, A., Meixner, T., Grunwald, S., Bishop, T., Diluzio, M., Srinivasan, R., 2006. A global sensitivity analysis tool for the parameters of multi-variable catchment models. *J. Hydrol.* 324 (1–4), 10–23.
- Wang, X., Kannan, N., Santhi, C., Potter, S.R., Williams, J.R., Arnold, J.G., 2011. Integrating apex output for cultivated cropland with swat simulation for regional modeling. *Trans. ASABE* 54 (4), 1281–1298.
- White, M.J., Santhi, C., Kannan, N., Arnold, J.G., Harmel, D., Norfleet, L., Allen, P., DiLuzio, M., Wang, X., Atwood, J., Haney, E., Vaughn Johnson, M., 2014. Nutrient delivery from the Mississippi River to the Gulf of Mexico and effects of cropland conservation. *J. Soil Water Conserv.* 69 (1), 26–40. <http://dx.doi.org/10.2489/jswc.69.1.26>.
- Williams, J.R., Arnold, J.G., Kiniry, J.R., Gassman, P.W., Green, C.H., 2008. History of model development at Temple, Texas. *Hydrolog. Sci. J.* 53 (5), 948–960. <http://dx.doi.org/10.1623/hysj.53.5.948>.
- Wu, L., Liu, S.S., Abdul-Aziz, O.I., 2012a. Hydrological effects of the increased CO₂ and climate change in the Upper Mississippi River Basin using a modified SWAT. *Clim. Change* 110, 977–1003. <http://dx.doi.org/10.1007/s10584-011-0087-8>.
- Wu, M., Demissie, Y., Eugene, Y., 2012b. Simulated impact of future biofuel production on water quality and water cycle dynamics in the Upper Mississippi river basin. *Biomass Bioenerg.* 41, 44–56.
- Yang, J., Reichert, P., Abbaspour, K.C., Xia, J., Yang, H., 2008. Comparing uncertainty analysis techniques for a SWAT application to the Chaohe Basin in China. *J. Hydrol.* 358 (1–2), 1–23.
- Zhang, Z., Wu, M., 2013. Evaluating the transport and fate of nutrients in large scale river basins using an integrated modeling system. In: Fu, B., Jones, K.B. (Eds.), *Landscape Ecology for Sustainable Environment and Culture*. Springer, Dordrecht, Heidelberg, Germany, pp. 187–204.